ON THE EFFECTS OF ROTOR ECCENTRICITY OF ROTATING MACHINES

A Dissertation
submitted in partial fulfilment
of the requirements for the Degree
of
MASTER OF ENGINEERING
in
ADVANCED ELECTRICAL MACHINES

By

RAMESH LAL JATANA

DEPARTMENT OF ELECTRICAL ENGINEERING
UNIVERSITY OF ROORKEE
ROORKEE
July, 1967

I N D E X

..../2

C E R T I F I C A T E

CERTIFIED that the dissertation entitled "ON THE EFFECTS OF ROTOR ECCENTRICITY OF ROTATING MACHINES" which is being submitted by Sri R.L. JATANA in partial fulfilment for the award of the degree of Master of Engineering in Advanced Electrical Machines of University of Roorkee, Roorkee is a record of student's own work carried out by him under my supervision and guidance. The matter embodied in this dissertation has not been submitted for the award of any other degree or diploma.

This is further to certify that he has worked for a period of 6 months from Jan. to June '67 for preparing dissertation for Master of Engineering at this University.

P. Mukhopadhyay

(P. MUKHOPADHYAY)
Professor in Electrical Engg.,
University of Roorkee,
Roorkee U.P.

Dated
July 17, 1967.

A C K N O W L E D G E M E N T S

The author is very much indebted to his respected Professor Dr. P. Mukhopadhyay for suggesting this topic for the discussion and wishes to express his deep sense of gratitude for his able guidance and affectionate encouragement throughout. He has been very kind enough in devoting much of his valuable time in helping at every stage of the work.

The author also wishes to thank Professor C.S. Ghosh, Head of the Electrical Engineering Department, University of Roorkee, Roorkee for various facilities offered in the department in connection with this work.

R. L. JATANA

NOMENCLATURE

B = Magnetic flux density

H = Magnetising force

ϕ = Magnetic potential function

ψ = Magnetic flux function

r, θ = Polar coordinate

r_1, r_2, θ_1, θ_2 = Bipolar coordinates defined in Fig. 2.2.

R_1 = Radius of rotor surface

R_0 = Radius of stator bore

ϵ = Eccentricity of rotor

δ = Nominal air-gap

δ_1 = Virtual air-gap

P = Number of pole pairs

P' = Permeance in the eccentric air gap.

= radius of rotor surface and stator bore in w-plane.

M' = Net air-gap m.m.f.

F_1 = U.M.P. = Unbalanced Magnetic Pull

q_r = Ratio of rotor deflection caused by the U.M.P. to the displacement causing the unbalanced pull

N_c = Critical speed

f = Gravity deflection in cms, caused under the static influence of rotor weight W.

W = weight of the rotor in Kilograms.

S U M M A R Y

A method of calculation is given for the determination of the magnetic field in the air gap of a machine without salient pole and with an eccentric rotor for various distribution of the ampere turns at the stator surface. The basic case of concentric rotor is considered first with simplified assumptions and the complex potential is derived at any point in the air gap.

The eccentric annulus representing the air gap when the rotor is displaced is related to a concentric annulus by means of conformal transformation. Hence the complex potential is known at any point in the eccentric air gap and the expressions are thence derived for the potential and the flux functions at any point in the air gap. Finally the expressions thus derived are used to calculate the radial magnetic field at the surface of an eccentric rotor.

The study is also made as to how the unbalanced magnetic forces occur, what is the magnitude of such forces and to what extent these influence the critical speed of the machine.

Finally the effect of eccentricity on noise is discussed in short and the method is given for the calculation of noise level due to high frequency fields produced by the displacement of rotor and stator centres.

INTRODUCTION

The knowledge of magnitude of the unbalanced magnetic pull occurring in eccentrically placed rotor in synchronous and asynchronous machine is an important factor for the design of the electrical machine because such forces can greatly influence the critical running speed of the machine. An unbalanced pull may be defined as the net side ways force between the stator and the rotor of the electrical machine resulting from a difference in the air- gap flux densities on the opposite sides of the machine. This difference in flux densities is generally caused by a difference in the air-gaps of two side. Many causes contribute to such a condition. Frequently the outer surface of the rotor and the inner surface of the stator are not perfectly cylindrical. Even if they are perfectly cylindrical and concentric while the machine is cold, a noticeable deviation may occur due to the difference in temperature between the stator and the bedplate when the machine is heated. With a machine of five meters diameter, for instance, a difference of 20°C in the average temperatures of frame and bedplate would correspond to approximately one mm. difference in length.

C H A P T E R 1

1. I N T R O D U C T I O N

11 REVIEW OF EARLIER WORK

INTRODUCTION

The knowledge of magnitude of the unbalanced magnetic pull occurring in eccentrically placed rotor in synchronous and asynchronous machine is an important factor for the design of the electrical machine because such forces can greatly influence the critical running speed of the machine. An unbalanced pull may be defined as the net side ways force between the stator and the rotor of the electrical machine resulting from a difference in the air- gap flux densities on the opposite sides of the machine. This difference in flux densities is generally caused by a difference in the air-gaps of two side. Many causes contribute to such a condition. Frequently the outer surface of the rotor and the inner surface of the stator are not perfectly cylindrical. Even if they are perfectly cylindrical and concentric while the machine is cold, a noticeable deviation may occur due to the difference in temperature between the stator and the bedplate when the machine is heated. With a machine of five meters diameter, for instance, a difference of 30°C in the average temperatures of frame and bedplate would correspond to approximately one mm. difference in length.

Another factor is the clearance between the shaft and bearings. While the machine is at rest, the oil is squeezed out from underneath the shaft, and all the clearance will be between the top part of the shaft and the upper bearing shell. In this position the machine is errected and centered. When the machine is running, the bearing is flooded with oil and clearance divides equally arround the shaft. Very frequently of course, imperfect errection, a bending of the shaft or slight subsidence of the foundations with consequent distortion of the bedplate may be the cause of a displacement of rotor and stator centres.

REVIEW OF EARLIER WORK:

Fisher-Hinnen[1] in his 'Dynamo Design' published in 1899 derives the following formula :-

$$\text{pull in dynes} = \left[\frac{B^2 A}{25 \times 10^6} \times \frac{\chi}{g \alpha} \right] C$$

Where

B = Flux density in the air-gap in lines per sq.cms.

A = Section of the pole face in sq. cms.

χ = Rotor displacement

g = Air-gap clearance

α = Ratio of the reluctance of the total magnetic circuit to that of the normal air-gap alone.

C = is a calculated coefficient, given in the following table.

Value of C	Number of poles	Remarks
2.0	4	Displacement along the field magnets.
2.8	4	Displacement along the neutral line.
6.0	6	Displacement along the axis of the magnet
9.0	8	Displacement along neutral line.
15.0	12	Displacement along neutral line.
20.0	16	Displacement along neutral line.

B.A. Behrend[2] in 1900, gives a mathematical discussion of the case of a machine with very large number of poles and derrives the formula :-

$$\text{Pull} = \frac{B^2 S'}{8\pi} \times \frac{2X}{g}$$

Where $S' = \pi R l = \frac{1}{2} \times$ Total air-gap area and shows that this is exactly one half the value obtained by assuming that half of the poles have a gap $(g-x)$ and the other half a gap $(g+x)$.

If we substitute for $S' = \frac{1}{2} \times A \times$ Poles, Behrend expression becomes :

$$\text{Pull} = \frac{B^2 A}{8\pi} \cdot \frac{X}{g} \times p$$

Edgar Knowlton[3], about the same time, derives an expression for a machine with definate number of poles and obtain the formula :-

$$\text{Pull in lbs.} = \left[\frac{B^2 A}{77,134,00} \times \frac{X}{g \alpha} \right] C$$

Where

B = Normal gap density in lines per sq. inch

A = Area of the pole face in sq. inch.

X = Displacement

g = Nominal air-gap

α = Ratio of the total reluctance of the Magnetic circuit to that of the normal gap alone.

C = Coefficient, obtained by calculation

= 2 for 4 poles

= 4.7 for 6 poles

= 7 for 8 poles

= 9.6 for 10 poles

Above 10 poles, C = No. of poles, and then the formula checks with that of Behrend. Knowlton's expression is of the same form as that of Fisher- Hinnen, but the constants given by the two authors for 6 and 8 poles differ considerably. Knowlton, moreover, states, that it makes little difference whether the plane of deflection is taken through a pole or between the two poles.

J. Rey[4], in 1904, states that Behrend's and Fisher- Hinnen's formulas are not consistent and sets out to derive a new formula especially applicable to induction motors with eccentric rotor. Rey's formula is :-

$$\text{Pull in dynes} = \frac{1}{8\pi^2} (B_{eff})^2 \; S \times C$$

$B_{eff.}$ = 1.1 $B_{av.}$ for Sine distribution of flux.

S = Rotor surface = $2\pi R l$

C = f (e)

e = eccentricity, expressed as a fraction in terms of the single air-gap = x / g.

and for

e = x/g	0.05	0.1	0.15	0.2	0.25	0.3	0.4
C	0.157	0.319	0.488	0.688	0.866	1.084	1.63

For an eccentricity less than 20 percent, this formula reduces to

$$= \frac{(B_{eff})^2}{8\pi} \times S \times \frac{x}{g} \quad \text{Approximately}$$

which is identical with Behrend's formula, because with a sine distribution of flux, as in induction motors, $(B_{eff})^2$ is the average value of B^2, where B is density at any point along the air - gap.

J.K. Sumec[5] derives a similar formula to that of Behrend and Rey, but by certain transformation reduces

it to the form: -

$$\text{Pull in dynes} = \frac{B^2}{8\pi} \times S \times \frac{X}{g} \quad \frac{1}{\left[1 - \left(\frac{X}{g}\right)^2\right]^{3/2}}$$

This is the same as Behrend's formula except for the last term which for an eccentricity as large as 25 percent, is equal to 1.1 or difference of only 10 percent, the correction term differs from unity by only one percent.

Sumec's formula, as might be expected, gives the same value as derived by Rey. It is to be noted that in most of the formulas derived mathematically, the effect of reluctance of the iron part of the magnetic circuit is neglected. The assumption made that the flux density is inversely proportional to the air-gap and is therefore only true in unsaturated machines.

In 1905, B. Soschinski[6] gives an account of some tests made to check the formulas of Rey and Sumec. Very good agreement was obtained for smaller air-gaps and iron feebly saturated, taking the area and flux density at the top of the teeth but with increasing saturation, the calculated result (iron reluctance neglected) were higher than experimental ones. With larger values of air-gap, however, the test values were throughout higher (upto 100 percent).

The latter result was accounted for by the fact that as the armature moves to one side the flux lines become concentrated at the tooth tip of the side of the reduced gap and spread out on the side of increased gap.

In the same year (1905), Niethammer[7] by a transformation of Sumei's equation obtains the following formula which permits taking into account the reluctance of the iron path by determining the flux density from the saturation curve. This expression is regarded by him as giving the most reliable results.

$$\text{Resultant Pull in Kg.} = \frac{1}{2}\left[\left(\frac{B_{max}}{3000}\right)^2 - \left(\frac{B_{min}}{3000}\right)^2\right] p \cdot A$$

C. R. Moore[8], in 1911, gives a graphical method of studying the unbalanced Magnetic Pull, by using Maxwell's formula and the given saturation curve of the machine, and summing up the pull for various adjacent halves of adjoining pole faces. He takes the air-gap density for these half ares as corresponding to the average air-gap lengths across these faces and to the given excitation. Upon plotting various field excitations he establishes that for low saturation the pull increases with the excitation; at a critical density, however, corresponding to about the knee of magnetization curve, the unbalanced pull reaches a maximum for all eccentricities, and for larger excitation decreases again. Therefore, a machine, which normally operates

at high saturation, may be subjected to a greater stresses while it is building up than under normal field excitation.

Miles Walker[9] in his book on 'Specification and Design of Dynamo-Electric Machinery' (1915), points out that the ammount of unbalanced pull for a given displacement will depend on the extent to which the iron parts are saturated, and that the effect of increased saturation is to reduce the pull for a given air-gap clearance and magnetic induction. He first assumes that all the ampere turns are expended in the air-gap and by the usual method derives an expression for the unbalanced pull exactly similar to that of Behrend. He then shows how the saturated magnetic circuit may be replaced by an equivalent air-gap obtained by means of a graphical construction on the saturation curve of the machine, and then uses this equivalent air-gap in the formula for the unbalanced pull.

Rosenberg[10] in 1918, investigates the occurrance and the effect of unbalanced pull in electrical machines and has derived some practical formulas for the use of the designer. He has studied the influence of saturation on the unbalanced pull for a given induction and found that in a given machine there is a "critical induction" which gives a higher unbalanced pull than any other smaller or larger induction. He gives a simple rule for

determining this critical induction and also investigate the permissible deflection of the machines parts in connection with the unbalanced pull, and the influence of the latter on the critical speed.

Robinson[11] in 1943, gives the formula for the calculation of unbalanced pull which takes into account the combined effects of saturation, parallels and primary reactance. He represents the no load saturation curve by a power equation of the form :-

$$i_m = e\, I_g + e^m\, I_s$$

Where,

- e = Voltage in p.u. corresponding to air-gap flux.
- I_g = Magnetising current for the air-gap at normal voltage.
- I_s = Magnetising current for saturation at normal voltage.
- i_m = Magnetising current at any voltage
- m = Saturation curve exponent defined by $i_s = e^m\, I_s$

Assuming a constant gap density over a section of the machine and considering that a constant change is made in the air-gap while the magnetising current is kept constant, he finds the expression for the resultant change in the gap density due to the rotor eccentricity, which is given by :-

$$b = \frac{1 - \left[\frac{K_g'}{K_c} \quad \frac{g - \Delta}{g}\right] \cdot B_g}{\frac{K_g'}{K_c} \quad \frac{g-\Delta}{g} + m\, e^{m-1} \frac{I_s}{I_g}}$$

Where

b = Rise in gap flux density

g = Single air-gap in inches

g' = Single air-gap when the rotor is displaced by $(g-\Delta)$ inches.

Δ = Amount of the rotor displaced from the center of the stator in inches.

K_c = Carter coefficient for an air-gap g

K_g' = Carter coefficient for an air gap g'

B_g = Air gap flux density at normal voltage in Kilo-lines per square inch.

If very small deflection is considered this equation has the following form :

$$b = K_s \frac{\Delta}{g} \cdot B_g$$

Where $K_s = \dfrac{1}{1 + m\, e^{m-1} \dfrac{I_s}{I_g}}$

K_s = Factor allowing for the effect of saturation on density rise.

The expression for unbalanced magnetic pull in Induction motor with a series or two parallel primary winding operating at any speed and voltage as given

Robinson is as follows :

$$U.M.P. = 0.01366 \; K_s \frac{\Delta}{g} \; e^2 \; B_g^2 \; A$$

In another form, this may be written as :

$$U.M.P. = \text{Constant} \times \frac{e^2}{1 + m \, e^{m-1} \frac{l_s}{l_g}}$$

Solving for a maximum :

$$E^{m-1} = \frac{2}{(m^2 - 3m) \frac{l_s}{l_g}}$$

Where E is the per unit voltage at which maximum pull occurs.

He further gives the expression for unbalanced pull with more parallels in the primary winding expressing it in the following form :

$$U.M.P. = 2.88 \, e^2 \; \frac{B_g^2 \, A}{g} \left[a \, K_s + (1-a) \, K_R \right] \times 10^{-4}$$

Where a = Factor depending upon the number of parallels.

K_R = Factor allowing for the effect of saturation and primary reactance on the density rise.

$$= \frac{1}{1 + m \, e^{m-1} \frac{l_s}{l_g} + \frac{1}{l_g \, X_1}}$$

X_1 = Stator leakage Reactance.

From this equation, it is practically impossible to solve analytically for the voltage at which maximum pull will occur. However, a close approximation is obtained, if we use in this formula the voltage at which the pull is a maximum, considering saturation alone.

With the constants that are used in most induction motors, the factor $\left[a K_s + (1-a) K_R \right]$ is approximately equal to K_s divided by the number of parallels. Therefore, the important fact which was established by Robinson is that the unbalanced pull for an induction motor having three or more parallels in the primary winding may be obtained approximately by calculating the pull for a series winding and then dividing by the number of parallels.

Covo[12], in 1954, derives the following formula for calculating the average unbalanced pull as well as its magnitude at different angular position of the rotor. This expression is regarded by him as giving the most reliable results for higher eccentric

$$P_{av} = \frac{\pi D W}{72.13 \times 10^{6}} B_m^2 C_{av}$$

Where

δ = Eccentricity in inches

α = Angle of the eccentricity = angle betwee
axis and th
centre lin
magnetic p

D = Diameter of average air gap in inches.

w = Length of rotor stackings.

Δ = Average mechanical air gap.

b = Number of poles.

B_m = Maximum gap flux density of motor with even air gap equal to Δ in lines per square inch.

$$C_{av} = \frac{1}{2\pi} \int_0^{2\pi} C_\alpha \, d\alpha$$

$$\text{and } C_\alpha = \frac{1}{2\pi \Psi_\alpha^2} \int_0^{2\pi} \frac{\left[\cos \frac{p}{2}(\theta + \alpha) - \beta_\alpha\right]^2 \cos\theta}{(1 - e\cos\theta)^2} \, d\theta$$

$$\beta_\alpha = \cos \frac{p}{2}\alpha \left[\frac{1 - \sqrt{1-e^2}}{2e}\right]^{p/2}$$

$$\Psi_\alpha = \frac{1}{4} \sum_{n=1}^{p} \left| \int_{(2n-3)\frac{\pi}{p} - \alpha}^{(2n-1)\frac{\pi}{p} - \alpha} \frac{\cos \frac{p}{2}(\theta + \alpha) - \beta_\alpha}{1 - e\cos\theta} \, d\theta \right|$$

The factor C_{av} is a function of effective relative eccentricity 'e' and the number of poles p. Curves of C_{av} as a function of e for various number of pole shows that the average pull P_{av} increases with increase in the number of poles and alternating component of pull decreases with increase of p.

The equations derived by Covo are applicable on the motors running at no load or very light loads. The results are not valid for heavy load conditions

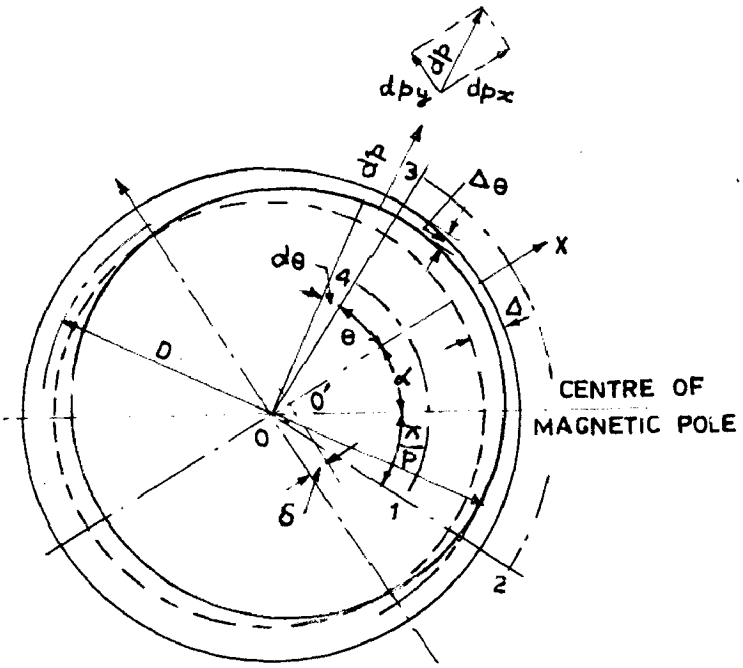

O _ CENTRE OF STATOR BORE
O' _ CENTRE OF ROTOR

FIG. 1.1

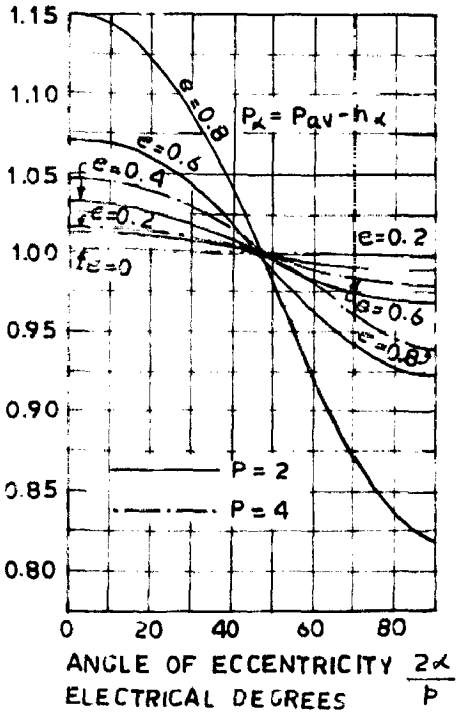

FIG.1 2.RESULTANT MAGNETIC PULL AS FUNCTION OF ANGLE OF ECCENTRICITY

since the effects of rotor currents and rotor skew were not taken into account in the calculation of air-gap flux distribution.

He further analyses the pulsating character of these forces. It is shown in Fig. 1.2. that the alternating component of the resultant force has a first harmonic of the form P' Cos p α . The space angle α will usually vary with time. He considers the two extreme cases:

i. STATIC ECCENTRICITY i.e., the rotor and the shaft are concentric to each other but the bearings are eccentric with respect to the stator bore, the rotor will rotate arround with its centre 'O' (Fig. 1.1). In such case angle α will be stationary with respect to the stator but will vary at synchronous speed with respect to the rotating field produced by the stator winding . Therefore the angle α is given by:-

$$\alpha = \frac{2}{p} \quad (2\pi f)\, t$$

Where f = Line frequency

t = Time in seconds.

Therefore the first harmonic of the magnetic pull (p_α) will be of the form P' Cos 2 $(2\pi f)t$. The fundamental frequency of p_α will be double line frequency.

ii. DYNAMIC ECCENTRICITY i.e. the bearings are concentric with respect to stator but the rotor is eccentric with respect to the shaft. The angle α will vary at slip frequency.

or $\alpha = \frac{2}{p} S (2\pi f)t.$

The fundamental frequency of P_α will now be double slip frequency.

Therefore the important fact which Covo establishes, is that the change in the magnitude of the resultant pull can be at double line frequency or double slip frequency according to the nature of eccentricity.

Friese and Jordan[13], in 1962, have studied the pull occurring on an eccentrically placed rotor in synchronous and asynchronous machines. Its effect on critical running speed and the effect of damping on its magnitude are also considered. An analogy is made between the pull and an electromagnetic spring having a negative coefficient to simulate the reduction in critical running speed which occurs.

The derive the formula for critical speed as

$$N_e = 300 \sqrt{\frac{C_K + C_e}{G_L}}$$

Where,

C_e = Electromagnetic spring number = F/ϵ

C_w = G_L / f'

G_L = Weight of rotor.

F = Magnetic pull

f' = Deflection of the rotor under the influence of its own weight.

C_w and C_e are expressed in Kilograms / cms.

C H A P T E R 2

CALCULATION OF MAGNETIC FIELD IN THE AIR GAP OF A NON SALIENT POLE MACHINES WITH ECCENTRIC ROTOR

2.1. In this Chapter, a method of calculation is developed for the determination of the magnetic field in the air-gap of an idealized machine without salient pole and with an eccentric rotor for various distributions of the ampere turns of the stator surface.

CASE 1a. FULL PITCH CONCENTRATED WINDING :

It is shown in equation (6) of the Appendix 1 that the m.m.f. distribution of a full pitch concentrated winding referring to the origin O' can be expressed as :

$$a = \frac{4M}{\pi} \sum_{n=0}^{\infty} (-1)^n \frac{\text{Cos } (2n+1)\,P\theta}{(2n+1)\,P} \qquad \ldots(2.1)$$

We shall now investigate the flux density distribution in the air-gap of the concentric rotor with the following assumptions:-

1. Saliency is neglected owing to excessive mathematical complexity.

2. Effect of magnetic saturation is ignored. This is partly due to the lack of mathematical relation between the magnetic intensity and the corresponding induction in the ferro-magnetic materials and, more especially, to the grave difficulty in taking accoun

of any such relation in the solution of the field equations.

3. The permeability of the rotor and stator materials are assumed to be infinite.

4. Effect of slots and ventilating ducts are also omitted again owing to the mathematical complexity.

5. The stator and the rotor are assumed to have smooth cylindrical iron surfaces and the length of the core is assumed to be larger in comparision with its diameter so that the problem can be treated as two dimensional one.

6. Two cases may be distinguished according as the stator core is assumed to have a finite or an unlimited radial depth. However, as will become apparent in the later section, only the latter condition is amenable to calculation when the rotor becomes eccentric, and consideration will therefore be limited to this case only.

The Maxwell's equations for calculating the magnetic field in the air-gap with concentric air-gap can be written as :

$$\text{Curl } H = 0 \qquad \ldots (2.2$$

$$\text{Div } B = 0 \qquad \ldots (2.3$$

Choosing the cylindrical polar coordinate systems of axes, equation nos. (2.2) and (.2.3) can be expressed as :

$$\frac{\partial H_\theta}{\partial r} + \frac{1}{r} H_\theta - \frac{1}{r} \frac{\partial H_r}{\partial \theta} = 0 \qquad ..(2.4)$$

$$\frac{\partial H_r}{\partial r} + \frac{1}{r} H_r + \frac{1}{r} \frac{\partial H_\theta}{\partial \theta} = 0 \qquad ...(2.5)$$

Where H_r = Radial component of the Magnetic field intensity.

H_θ = Tangential component of the Magnetic field intensity.

Differenciating equation No. (2.4) with respect to θ ,

$$\frac{\partial^2 H_\theta}{\partial r \, \partial \theta} + \frac{1}{r} \frac{\partial H_\theta}{\partial \theta} - \frac{1}{r} \frac{\partial^2 H_r}{\partial \theta^2} = 0 \qquad ...(2.6)$$

From equation No. 2.5, we have

$$\frac{1}{r} \frac{\partial H_\theta}{\partial \theta} = - \frac{\partial H_r}{\partial r} + \frac{1}{r} H_r \qquad ...(2.7)$$

and $$\frac{\partial^2 H_\theta}{\partial r \, \partial \theta} = - r \frac{\partial^2 H_r}{r^2} + 2 \frac{\partial H_r}{\partial r} \qquad ...(2.8)$$

From Equations No. (2.6), (2.7) and (2.8) , we have

$$r \frac{\partial^2 H_r}{\partial r^2} + 3 \frac{\partial H_r}{\partial r} + \frac{1}{r} H_r + \frac{1}{r} \frac{\partial^2 H_r}{\partial \theta^2} = 0 \qquad ...(2.9)$$

The above equation represents the field of the air gap which can be solved by the method of separation of variables:

Assuming, as usual, the solution of equation (2.9) of the form

$$H_r = R(r) \quad \textcircled{H}(\theta) \qquad \ldots(2.10)$$

The independent variables are separated and equation No. (2.9) is replaced by :-

$$r^2 \frac{d^2R}{dr^2} + 3r \frac{dR}{dr} + 1 - (2n+1)^2 p^2 R = 0 \qquad \ldots(2.11)$$

and $$\frac{d^2\textcircled{H}}{d\theta^2} + (2n+1)^2 p^2 \theta = 0 \qquad \ldots(2.12)$$

Where $n = 0, 1, 2, 3, 4 \ldots\ldots$

Since the variation of $\textcircled{H}$ is of the form

$$\sum_{n=0}^{\infty} \frac{\cos (2n+1) P\theta}{(2n+1) P}$$

By means of the substitution $R = e^{mx}$, where $e^x = r$, equation No. (2.11) is reduced to the form -

$$\frac{d^2R}{dx^2} + 2\frac{dR}{dx} + 1 - (2n+1)^2 p^2 R = 0$$

Which has the solution

$$R = C_n r^{(2n+1)p-1} + D_n r^{-(2n+1)p-1}$$

The solution of Equation (2.12) is -

$$= A_n \cos (2n+1) P\theta + B_n \sin (2n+1) P\theta$$

Hence the solution of Equation No. (2.9) is given by

$$H_r = C_n r^{(2n+1)p-1} + D_n r^{-(2n+1)p-1}$$

$$A_n \cos (2n+1) P\theta + B_n \sin (2n+1) P\theta \qquad \ldots(.$$

From equation No. (2.9), we have

$$H_\theta = -\int \left(r \frac{\partial H_r}{\partial r} + H_r \right) d\theta \qquad \ldots (2.14)$$

From equation No. (2.13) and (2.14) we get

$$H\theta = -\left[C_n r^{(2n+1)P-1} - D_n r^{-(2n+1)P-1} \right] \left[A_n \sin (2n+1)P\theta - D_n \cos (2n+1)P\theta \right] + K \qquad \ldots (2.15)$$

Where K = constant of integration. But as the excitation is harmonic, the tangential and normal component of the magnetic field intensity should also be harmonic. Hence the constant K vanishes automatically.

2.1.1 BOUNDARY CONDITIONS :

1. Ampere turns distribution at the stator surface

$$i_n = \frac{4I}{\pi} \sum_{n=0}^{\infty} (-1)^n \frac{\cos (2n+1)P\theta}{(2n+1)P}$$

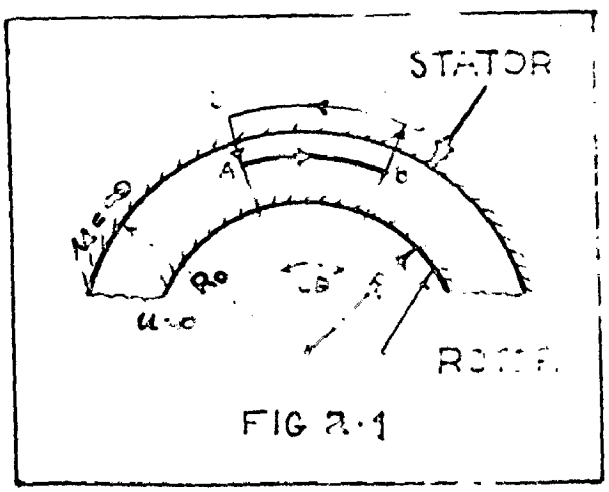

FIG 2.1

Referring to Fig. (2.1), consider the elemental path ABCD at the boundary surface between stator and the air-gap. The side BC and DA are small as compared to the side AB and CD, so BC and DA does not require m.m.f.

Also $AB = R_o \, d\theta$

$\therefore$ Total ampere turns $= H_\theta \, R_o \, d\theta$

$=$ Total current enclosed

$= d\,(A.T)$

$$\therefore \quad H_\theta\Big|_{r=R_o} = \frac{1}{R_o}\frac{d}{d_\theta}\left[\frac{4M}{\pi}\sum_{n=0}^{\infty}(-1)^n\frac{\text{Cos}\,(2n+1)P\theta}{(2n+1)P}\right]$$

$$\text{or} \quad H_\theta\Big|_{r=R_o} = -\frac{4M}{\pi R_o}(-1)^n \,\text{Sin}\,(2n+1)\,p\theta \qquad \ldots(2.16)$$

From equations No. (2.15) and (2.16), we have

$$-\left[C_n R_o^{(2n+1)P-1} - D_n R_o^{-(2n+1)P-1}\right]\times$$

$$\left[A_n \,\text{Sin}\,(2n+1)P\theta - B_n \text{Cos}\,(2n+1)P\theta\right]$$

$$= -\frac{4M}{\pi R_o}(-1)^n \,\text{Sin}\,(2n+1)P\theta$$

Since this is independent of θ, the coefficients of Cosine and Sine terms can be compared on both sides of the above equation, which gives

$$B_n = 0$$

$$\left[C_n R_o^{(2n+1)P-1} - D_n R_o^{-(2n+1)P-1} \right] = \frac{4M}{\pi R_o} (-1)^n \quad \ldots(2.17)$$

ii. Since the permeability of the rotor is infinity, tangential component of the magnetic field intensity at the roter surface vanishes:

$$\text{i.e.} \quad \left[C_n R_i^{(2n+1)P-1} - D_n R_i^{-(2n+1)P-1} \right] = 0$$

$$\text{or} \quad C_n = D_n R_i^{-2(2n+1)P} \quad \ldots(2.18)$$

From equations No. (2.17) and (2.18), we have

$$D_n = (-1)^n \frac{4M/\pi}{\left[\frac{R_o}{R_i}\right]^{(2n+1)P} - (R_o)^{-(2n+1)P}} \quad ..(2.19)$$

$$C_n = (-1)^n \frac{\frac{4M}{\pi} R_i^{-(2n+1)2P}}{\left[\frac{R_o}{R_i}\right]^{(2n+1)P} - (R_o)^{-(2n+1)P}} \quad ..(2.20)$$

The equations No. (2.13) and (2.14) are reduced to the form:

$$H_r = \sum_{n=0}^{\infty} \left[C_n r^{(2n+1)P-1} + D_n r^{-(2n+1)P-1} \right] \text{Cos } (2n+1)P\theta \quad ..(2.21)$$

$$H_\theta = \sum_{n=0}^{\infty} - \left[C_n r^{(2n+1)P-1} - D_n r^{-(2n+1)P-1} \right] \text{Sin } (2n+1)P\theta \quad ..(2.22)$$

2.2.4. EFFECT OF ROTOR ECCENTRICITY

The assumptions are same as with the concentric rotor considered above.

A difficulty, however, arises in the determination of the constants C_n and D_n by aid of conditions of continuity. The simplicity of calculating these constant in the concentric annulus is due to the fact that the radius vector at any point on the boundary surface coincides with the normal at that point and consequently the normal induction is governed by the potential gradient in the direction of the radius vector. Hence the analytical expression for the normal induction and like-wise for the tangential intensity, at ultimately coincident points on either side of the boundary is immediately obtained as the appropriate partial derrivative of the potential function concerned.

This simplicity of expression disappears when the annular air-gap becomes eccentric. If the origin of the polar coordinates is taken in the axis of the stator Core, the expression of a normal or of a tangential component of either magnetic induction or intensity at a point on the rotor surface takes the form of combination of both radial and circumferential components resolved along the tangent or normal at the point concerned. The expression of these resolutes involves the angle between the normal and the radius vector at any point and analytical complexit

are thereby introduced.

In order to overcome this difficulty the method of conformal transformation will be used to re-map the field in a-n eccentric annulus on a concentric annulus in another plane. The potential function at any point in the eccentric air-gap may then be deduced from the corresponding result with a concentric gap.

2.1.3. CONFORMAL REPRESENTATION OF AN ECCENTRIC ANNULUS ON A CONCENTRIC ANNULUS

Since the permeability of the rotor and stator are assumed to be infinite, the field in the gap immediately adjacent to all points on either the rotor or stator surface must be normal to these surfaces, which are, therefore, equipotential surfaces. Thus the magnetic field in the air-gap is bounded by equipotential surfaces, represented on a two dimensional diagram by a pair of eccentric circles S_1 and S_2 in Fig. (2.2) and the lines of force crossing the gap must meet S_1 and S_2 normally.

It may be shown by elementary geometry that there exists a family F of circles, represented by S_3, having their centres on the radical axis of S_1 and S_2 and having the properties of :-

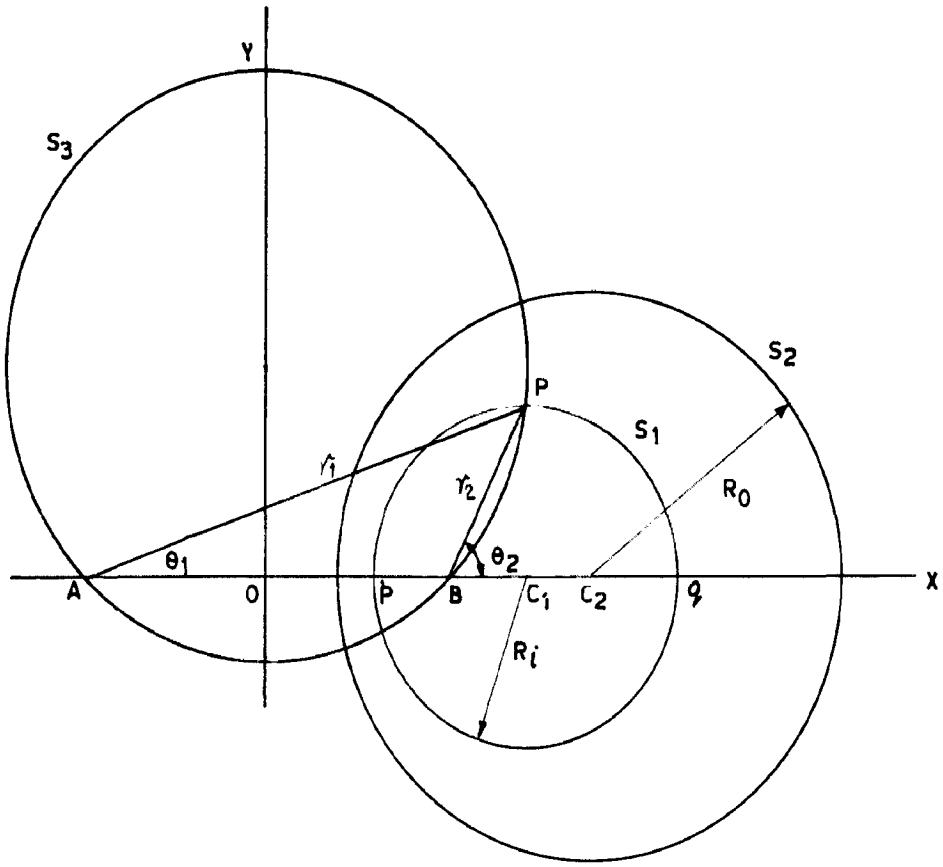

FIG.2.2.EQUIPOTENTIAL LINES IN AN ECCENTRIC AIR GAP

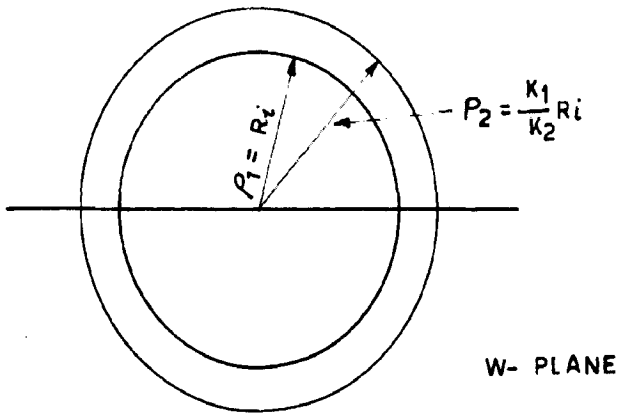

FIG.2.3.CONFORMAL REPRESENTATION OF AN ECCENTRIC RING IN THE Z-PLANE BY A CONCENTRIC RING IN THE W-PLANE

a. Intersecting S_1 and S_2 at right angles and (b) passing through the limiting points A and B of the coaxial system F' of circles containing S_1 and S_2. This family F is also orthogonal to all other members of the system F', so that F and F' form an orthogonal net in the space between S_1 and S_2 and therefore represent the possible systems of equipotential lines and lines of force respectively.

It is shown in Appendix '3' that

$$\frac{r_1}{r_2} = \text{Constant on } S_1 = K_1 \text{ (say)} \qquad \ldots(2.23)$$

Also

$$\left.\begin{aligned} r_1^2 &= (x+m)^2 + y^2 \\ r_2^2 &= (x-m)^2 + y^2 \end{aligned}\right\} \qquad \ldots(2.24)$$

From equation No. 2.23 and 2.24 we have

$$\frac{(x+m)^2 + y^2}{(x-m)^2 + y^2} = K_1^2$$

$$\text{or} \quad \left(x - m\frac{K_1^2+1}{K_1^2-1}\right) + y^2 = \left[\frac{2K_1 m}{K_1^2-1}\right]^2 \qquad \ldots(2.25)$$

The above expression is the equation of S_1, when referred to axes Ox and Oy.

$$\therefore \quad R_1 = \frac{2K_1 m}{K_1^2 - 1} \qquad \ldots(2.26)$$

$$x_1 = OC_1 = m\frac{K_1^2+1}{K_1^2-1} \qquad \ldots(2.27)$$

It is shown in Appendix (4) that

$$x_1 = \frac{1}{2}\left[\frac{R_0^2 - R_1^2}{\lambda} - \lambda\right] \qquad \ldots(2.28)$$

and also

$$x_2 = OC_2 = \frac{1}{2}\left[\frac{R_0^2 - R_1^2}{\lambda} + \lambda\right] \qquad \ldots(2.29)$$

Where λ denotes the distance C_1C_2 in Fig. (2.3) i.e. the eccentricity.

Hence $$m^2 = \frac{1}{4}\left[\frac{R_0^2 - R_1^2}{\lambda} - \lambda\right]^2 - R_1^2 \qquad \ldots(2.30)$$

The equation of the circle S_3 is obviously

$$\theta_2 - \theta_1 = \text{Constant on } S_3$$

$$= L \quad (\text{Say}) \qquad \ldots(2.31)$$

The system of coaxial circles including S_1 and S_2 may by a conformal transformation be represented by a system of concentric circles in another plane. Thus the bilinear transformation:-

$$w = k\,\frac{z-b}{z-a} \qquad \ldots(2.32)$$

Converts a circle in the z- plane into a circle in the w - plane.

A circle passing through the points $z_1 = a$, $z_2 = b$ in the z- plane therefore becomes a circle passing through the corresponding points $w_1 = \infty$ $w_2 = 0$ in the w - plane, i.e., a straight line through the origin. If now the points z_1, z_2 in the

z- plane are identified with the points A , B in Fig. 2.2 , the lines of force, typified by S_3 , become transformed into a pencil of straight lines through the origin in the w - plane. Thus the origin z being at 0 in Fig. 2.2.

$$a = -m \quad ; \quad b = m$$

and the relation (2.32) becomes

$$w = k \frac{z-m}{z+m} \qquad \ldots(2.33)$$

By this transformation the equipotentials, typified by S_1 and S_2 in Fig. 2.2, are transformed into a system in the w - plane[Fig(2.3)] orthogonal to this pencil of straight lines, i.e., a system of concentric circles having their common centre at the origin.

By virtue of equation No. (2.33) the points in the w- plane corresponding to points p and q in Fig. 2.2, i.e., the z - plane , are

$$w_p = k \frac{x_1 - R_1 - m}{x_1 - R_1 + m}$$

$$w_q = k \frac{x_1 + R_1 - m}{x_1 + R_1 + m}$$

These are both real quantities, if k is real, and the corresponding point must therefore lie on the real axis in the w- plane. Since the centre of the circle on which these points lie is at the origin, it follows that the diameter of this circle is given

Fig (2.2) is then

$$\rho_2 = \frac{k}{K_2} = \frac{K_1}{K_2} R_1 \qquad \ldots(2.39)$$

$$\text{Where } K_2 = \frac{m}{R_0} + \left[\left[\frac{m}{R_0}\right]^2 + 1 \right]^{1/2} \qquad \ldots(2.40)$$

The value of ρ_2 varies with m and hence with the eccentricity, from equation No. (2.39). For zero eccentricity it is easily shown that $\rho_2 = R_0$, and with maximum eccentricity, i.e. complete 'pull over', it is found that $\rho_2 = R_1$, so that the concentric air-gap in the w- plane shrinks to a circle of radius R_1.

Thus it has been shown that the conformal transformation represented by equation No. (2.38) maps the eccentric annulus of radii R_1, R_0 ($R_0 > R_1$) in the z- plane on a concentric annulus in the w-plane with centre at the origin and radii, R_1, $(\frac{K_1}{K_2}) R_1$, where $K_1 > K_2$.

2.1.4. COMPLEX POTENTIAL IN THE AIR-GAP OF AN IDEALIZED MACHINE WITH CONCENTRIC ROTOR

For the purpose of making use of the transformation discussed above, it is necessary to consider the complex potential function $\Phi + j\Psi$ and to express this as a function of complex variable z. Lines of equipotential and lines of force are characterized by constant value of Φ and Ψ respectively.

From equation No. (2.41) and (2.42), the complex potential in the air gap with concentric rotor is given by

$$\phi + j\psi = -\left[C_n' r^{(2n+1)P} - D_n' r^{-(2n+1)P}\right] \text{Cos } (2n+1)P\theta - j\left[C_n' r^{(2n+1)P} - D_n' r^{-(2n+1)P}\right] \text{Sin } (2n+1)P\theta$$

$$\phi + j\psi = -\left[C_n' (z)^{2n+1)P} - D_n' (z)^{-(2n+1)P}\right] \quad \ldots (2.43).$$

where $z = r \text{Cos } \theta + j\, r \text{Sin } \theta = r e^{j\theta}$

2.1.5. COMPLEX POTENTIAL IN THE AIR GAP OF AN IDEALIZED MACHINE WITH ECCENTRIC ROTOR

The eccentric air gap may be located in the z- plane and re-mapped as a concentric gap in the w- plane by means of conformal transformation expressed in equation (2.38). The complex potential at any point in the concentric air gap is given by equation (2.43) on replacing z by w .

i.e. $$\phi + j\psi = -\left[C_n' (w)^{(2n+1)P} - D_n' (w)^{-(2n+1)P}\right] \ldots (2.44)$$

The expression thus obtained also gives the complex potential at any point z in the eccentric air-gap, if z is replaced to w by equation (2.38) The origin of z being at 'O' in Fig. (2.2) and the

The component of magnetic field intensity in any direction is given by the negative potential gradient in that direction.

$$\therefore \quad H_r = -\frac{\partial \phi}{\partial r} \quad , \text{ and } H_\theta = -\frac{1}{r}\frac{\partial \psi}{\partial \theta}$$

From equation No. (2.21), we have

$$\frac{\partial \phi}{\partial r} = -\left[C_n r^{(2n+1)P-1} + D_n r^{-(2n+1)P-1}\right] \text{Cos } (2n+1)P\theta$$

$$\therefore \quad \phi = -\left[C'_n r^{(2n+1)P} - D'_n r^{-(2n+1)P}\right] \text{Cos } (2n+1)P\theta \qquad \ldots (2.41)$$

$$\text{Where } C'_n = \frac{C_n}{(2n+1)P} \quad , \quad D'_n = \frac{D_n}{(2n+1)P}$$

Since ϕ and ψ are conjugate function defining the function $f(z)$. From Cauchy Riemann equation, we have

$$\frac{\partial \phi}{\partial r} = \frac{1}{r}\frac{\partial \psi}{\partial \theta} \quad \text{and} \quad \frac{\partial \phi}{\partial \theta} = -r\frac{\partial \psi}{\partial r}$$

$$\therefore \quad \frac{1}{r}\frac{\partial \psi}{\partial \theta} = -\left[C_n r^{(2n+1)P-1} + D_n r^{-(2n+1)P-1}\right] \text{Cos}(2n+1)P$$

$$\psi = -\left[C'_n r^{(2n+1)P} + D'_n r^{-(2n+1)P}\right] \text{Sin}(2n+1)P\theta \qquad \ldots (2.42)$$

(The integration constant is ignored since the total potential will be differenciated to determine the magnetic field intensity).

origin of w being at the centre of the rotor.

The complex potential function at any point 's' in the eccentric air-gap is given by

$$\phi + j\psi = -\left[C_n' \left(k \frac{z-m}{z+m} \right)^{(2n+1)P} - D_n' \left(k \frac{z-m}{z+m} \right)^{-(2n+1)P} \right]$$

The above expression can be resolved into real and imaginary parts by the aid of the following identities -

$$\left(\frac{z-m}{z+m}\right)^{n} = \left(\frac{r_2}{r_1}\right)^{n} \left[\text{Cos } n(\theta_2 - \theta_1) + j \text{ Sin } n(\theta_2 - \theta_1) \right]$$

$$\left(\frac{z-m}{z+m}\right)^{-n} = \left(\frac{r_1}{r_2}\right)^{n} \left[\text{Cos } n(\theta_2 - \theta_1) - j \text{ Sin } n(\theta_2 - \theta_1) \right]$$

$$\therefore \quad \phi = -\sum_{n=0}^{\infty} \left[C_n' \left(\frac{k}{K}\right)^{(2n+1)P} - D_n' \left(\frac{k}{K}\right)^{-(2n+1)P} \right] \text{Cos } (2n+1)PL \qquad \ldots (2.45)$$

$$\psi = -\sum_{n=0}^{\infty} \left[C_n' \left(\frac{k}{K}\right)^{(2n+1)P} + D_n' \left(\frac{k}{K}\right)^{-(2n+1)P} \right] \text{Sin } (2n+1)PL \qquad \ldots (2.46)$$

2.1.6. DETERMINATION OF THE COORDINATES (K, L) OF ANY POINT IN THE ECCENTRIC GAP

If (r , θ) be the polar coordinate referred to pole C_1 (i.e the centre of the rotor) and the initial line AOB of Fig. 2.2 of a point in the eccentric air-gap. Then

Since $\frac{dK}{dS_1} = 0$

Similarly H_2 , the component of the intensity in the direction of dS_2 , is given by :-

$$H_2 = -\frac{\partial\phi}{\partial S_2}$$

$$= -\left[\frac{\partial\phi}{\partial K}\frac{dK}{dS_2} + \frac{\partial\phi}{\partial L}\frac{dL}{dS_2}\right]$$

$$= -\frac{\partial\phi}{\partial K}\frac{dK}{dS_2} \qquad \ldots(2.50)$$

Since $\frac{dL}{dS_2} = 0$

It is shown in Appendix (6) that $\frac{dK}{dS_2}$ and $\frac{dL}{dS_1}$ are given by

$$\frac{dK}{dS_2} = -\frac{2m}{r_2^2} \qquad \ldots(2.51)$$

$$\frac{dL}{dS_1} = \frac{2m}{K r_2^2} \qquad \ldots(2.52)$$

Since the family of the curves represented by K = Constant and L = Constant are orthogonal. Hence the resultant magnetic intensity at any point in the gap is

$$H = (H_1^2 + H_2^2)^{1/2}$$

$$= \left[\left\{\frac{\partial\phi}{\partial L}\frac{dL}{dS_1}\right\}^2 + \left\{\frac{\partial\phi}{\partial K}\frac{dK}{dS_2}\right\}^2\right]^{1/2} \qquad \ldots(2.53)$$

$$r_1 e^{j\theta_1} = x_1 + m + r e^{j\theta}$$

$$r_2 e^{j\theta_2} = x_1 - m + r e^{j\theta}$$

$$\therefore \frac{r_1}{r_2} e^{j(\theta_1 - \theta_2)} = K e^{-jL} = \frac{x_1 + m + r e^{j\theta}}{x_1 - m + r e^{j\theta}}$$

It is shown in Appendix 5 (a) that

$$K = \frac{(m + x_1)^2 + 2(m + x_1) r \cos\theta + r^2}{\left[(R_1^2 + r^2 + 2 x_1 r\cos\theta)^2 + (2mr\sin\theta)^2\right]^{1/2}} \quad \ldots(2.47)$$

and $$L = \tan^{-1} \frac{2 mr \sin\theta}{R_1^2 + r^2 + 2 x_1 r \cos\theta} \quad \ldots(2.48)$$

2.1.7. MAGNETIC FIELD INTENSITY IN AN ECCENTRIC AIR GAP

The component of magnetic field intensity in any direction is given by the negative potential gradient in that direction. Thus let dS_1 and dS_2 denote elements of arc of the curves K = Constant and L = Const passing through any point in the gap. Then H_1, the component of intensity in the direction of dS_1 is given by

$$H_1 = - \frac{\partial\phi}{\partial S_1}$$

$$H_1 = - \frac{\partial\phi}{\partial K} \frac{dK}{dS_1} + \frac{\partial\phi}{\partial L} \frac{dL}{dS_1}$$

$$H_1 = - \frac{\partial\phi}{\partial L} \frac{dL}{dS_1} \quad \ldots(2.49)$$

The direction of H is, of course, normal to the equipotential curve through the point considered. The direction of the component H_3 at any point is tangential to the curve L = Constant, passing through the point, and is therefore always normal to the surface of either the rotor or the stator. Since these are assumed to be equipotentials, it follows that the resultant air-gap intensity, at either its inner or outer boundary, is given by equation (2.30).

2.1.8. EFFECT OF FINITE RADIAL DEPTH OF STATOR

As stated in the assumptions, the foregoing analysis has been restricted to a stator of unlimited radial depth. The reason for this is that, although the conformal transformation (2.30) maps the eccentric air-gap in the z - plane as a concentric annulus in the w- plane, the same transformation maps the concentric annulus representing the stator core as an eccentric annulus in the v - plane. A concentric stator ring in the w- plane would correspond to an eccentric ring in the z - plane bounded externally by a circle coaxial with the circles S_1 and S_2 in Fig. (2.2)

It might appear superficially that this difficulty could be overcome by the device of using a mapping function for the stator different from that given by equation (2.30) and such that the actual

stator ring is represented in the w - plane by annulus concentric with that representing the eccentric air-gap, and the internal diameter of re-mapped stator is the same as the external diameter of the re-mapped air - gap, such a mapping function for the stator is evidently

$$w = \left(\frac{f_2}{R_0}\right)(z - x_2)$$

as can be seen from Fig. (2.2).

However, while equation (2.38) gives a conformal transformation of the air-gap and the above suggested formula gives a conformal transformation of the stator, there is not a conformal transformation of the field at the boundary between stator and the air-gap. This is due to the fact that the direction of the field at any point on the stator side of this boundary is determined by the direction of the field in the air-gap adjacent in conjuction with the law of 'magnetic refraction' incorporating the boundary conditions on magnetic induction and on magnetic intensity. Consequently an arbitrary mapping function such as suggested above when applied to the stator ring in the z- plane will not, in general, give the correct intensity and orientation to the field in the stator at points on the boundary, and therefore elsewhere, when the air-gap field is re-mapped by equation No. (2.38). It is therefore evident that equation (2.38) must be used

to give a conformal transformation of entire field from the z- plane to w- plane.

2.10. CALCULATION OF MAGNETIC FIELD AT THE SURFACE OF AN ECCENTRIC ROTOR

From equation No. (2.30) and (2.31), we have

$$H_\theta = \frac{2n}{r_2^{2n}} \frac{\partial \phi}{\partial K} \qquad \ldots (2.34)$$

Also from equations No. (2.34) and (2.43), we have

$$H_\theta = \frac{2n}{K r_2^{2n}} \sum_{n=0}^{\infty} \left[C_n \left(\frac{K}{K}\right)^{(2n+1)\beta} + D_n \left(\frac{k}{K}\right)^{(2n+1)\beta} \right] \cos(2n+1)\beta L$$

$$\ldots (2.35)$$

On account of conformal transformation, we have

$$R_1 = \rho_1 \quad , R_2 = \rho_2 = \frac{K_1}{K_2} R_1 \qquad \ldots (2.36)$$

$$\text{and} \qquad k = K_2 R_1$$

(K, L) are calculated from equations No. (2.47) and (2.48). Since the present calculation refers to the surface of the rotor, L is obtained by putting $r = R_1$ in equation (2.48), thus giving

$$\bar{\psi} = \tan^{-1} \frac{n \sin \theta}{R_1 + n_1 \cos \theta} \qquad \ldots (2.37)$$

K is equal to K_1 at the rotor surface and is shown in Appendix 3 (b).

And from Fig. (2.2), we can express the value of r_2 as

$$r_2 = \left[(R_1 \sin\theta)^2 + (x_1 - m + R_1 \cos\theta)^2 \right]^{1/2} \quad ..(2.58)$$

From Equations (2.19), (2.20) &2.55) and (2.56), we have

$$H_2 = \frac{16\, m\, M}{K_1 r_2^2 \pi} \sum_{n=0}^{\infty} \frac{1}{\left[\frac{K_1}{K_2}\right]^{(2n+1)P} - \left[\frac{K_1}{K_2}\right]^{-(2n+1)P}} \cos(2n+1)P\,L$$

$$\ldots.(2.59)$$

The radial component of he flux density is given by

$$B_\theta = \mu_o H_2 \quad \ldots(2.60)$$

From equations (2.57), (2.58), (2.59) and (2.60), we have

$$B_\theta = F \times \sum_{n=0}^{\infty} \frac{\cos(2n+1)P \left[\tan^{-1} \frac{m \sin\theta}{R_1 + x_1 \cos\theta} \right]}{\left[(R_1 \sin\theta)^2 + (x_1 - m + R_1 \cos\theta)^2 \right]}$$

$$\ldots(2.61)$$

Where F is given by

$$F = \frac{16\, m\, M \mu_o}{\pi K_1} \sum_{n=0}^{\infty} \frac{1}{\left[\frac{K_1}{K_2}\right]^{(2n+1)P} - \left[\frac{K_1}{K_2}\right]^{-(2n+1)P}}$$

$$\ldots(2.62)$$

2.2.0 FRACTIONAL PITCH CONCENTRATED WINDING

It is shown in Equation (10) of Appendix 1 that the ampere turns distribution of the fractional pitch

concentrated winding can be expressed as

$$a = \frac{4M}{\pi} \sum_{n=0}^{\infty} (-1)^n \frac{\text{Cos } (2n+1)\,P\gamma \text{ Cos } (2n+1)P\theta}{(2n+1)\,P} \qquad \ldots (2.63)$$

The radial component of the flux density in the eccentric air-gap can be calculated exactly in the similar manner as that of full pitch concentrated coil, which on simplification gives:-

$$B_\theta = F \times \sum_{n=0}^{\infty} \frac{\text{Cos } (2n+1)\,P\gamma \text{ Cos } (2n+1)P \left[\text{Tan}^{-1} \frac{m \text{ Sin}\theta}{R_1 + x_1 \text{Cos}\theta}\right]}{(R_1 \text{Sin}\,\theta)^2 + (x_1 - m + R_1 \text{Cos}\,\theta)^2} \qquad \ldots (2.64)$$

F is given by Equation (2.62).

2.3. STEPPED DISTRIBUTION

The winding is distributed in the slots in the manner indicated in the lower part of Fig. 1-C of Appendix 1. It is shown in Equation (18) of Appendix 1, that the amperetturns distribution of such an arrangement can be expressed as :-

$$a = \frac{4M}{\pi} \sum_{n=0}^{\infty} (-1)^n \frac{\text{Sin}\left[q \frac{(2n+1)P\gamma}{2}\right] \text{Cos}\left[(q-1)(2n+1)\frac{P\gamma}{2}\right] \text{Cos}(2n+1)P\theta}{q \text{ Sin}\left[\frac{(2n+1)P\gamma}{2}\right] \qquad (2n+1)P} \qquad \ldots (2.65)$$

The radial component of flux density corresponding to this m.m.f. distribution is given by

$$B_\theta = F \times \sum_{n=0}^{\infty} \frac{\dfrac{\sin\left[q\,\frac{(2n+1)P\gamma}{2}\right]\cos\left[\frac{(q-1)(2n+1)P\gamma}{2}\right]}{q\sin\left[\frac{(2n+1)P\gamma}{2}\right]}}{(R_1\sin\theta)^2 + (x_1 - m + R_1\cos\theta)^2} \times \cos(2n+1)P\left[\tan^{-1}\frac{m\sin\theta}{R_1 + x_1\cos\theta}\right] \quad \ldots(2.66)$$

(ii) The winding is distributed in slots with the outer coil of less than full pitch (Fig. 1-E of Appendix 1), but with all the coils having the same number of turns. From equations No. 21 of Appendix 1, we have,

$$a = \frac{4M}{\pi} \sum_{n=0}^{\infty} (-1)^n \frac{\sin\left[q\,\frac{(2n+1)P\gamma}{2}\right]}{q\sin\frac{(2n+1)P\gamma}{2}} \cos(2n+1)P\left[\theta + \frac{q-1}{2}\gamma\right] \times \frac{\cos(2n+1)P\theta}{(2n+1)P} \quad \ldots(2.67)$$

and

$$B_\theta = F \times \sum_{n=0}^{\infty} \frac{\dfrac{\sin\left[\frac{q(2n+1)P\gamma}{2}\right]}{q\sin\left[\frac{(2n+1)P\gamma}{2}\right]}\cos(2n+1)P\left[\theta + \frac{q-1}{2}\gamma\right]}{(R_1\sin\theta)^2 + (x_1 - m + R_1\cos\theta)^2} \times \cos(2n+1)P\left[\tan^{-1}\frac{m\sin\theta}{R_1 + x_1\cos\theta}\right] \quad \ldots(2.68)$$

2.4. TRAPEZOIDAL DISTRIBUTION - FULL PITCH TYPE

From equation (2$) of Appendix i, the m.m.f. distribution of this type of arrangement can be expressed as

$$a = \frac{4M}{\pi\beta} \sum_{n=0}^{\infty} (-1)^n \frac{\text{Sin } (2n+1)P\beta}{(2n+1)^2 P^2} \text{Cos } (2n+1) P\theta \qquad \ldots(2.69)$$

$$B_\theta = F \times \sum_{n=0}^{\infty} \frac{\dfrac{\text{Sin } (2n+1)P\beta}{\beta (2n+1)P} \text{Cos}(2n+1)P \left[\text{Tan}^{-1} \dfrac{m\text{Sin } \theta}{R_1 + x_1 \text{Cos}\theta}\right]}{(R_1 \text{Sin } \theta)^2 + (x_1 - m + R_1 \text{Cos } \theta)^2} \qquad \ldots(2.70)$$

(ii) TRAPEZOIDAL DISTRIBUTION - FRACTIONAL PITCH TYPE

From Equation (2$) of Appendix i, the m.m.f. distribution of this arrangement of winding can be expressed as

$$a = \frac{8M}{\pi\beta} \sum_{n=0}^{\infty} (-1)^n \frac{\text{Sin } (2n+1)\frac{\beta}{2} \text{Cos}(2n+1)P(\theta + \frac{\beta}{2}) \text{Cos}(2n+1)P\theta}{(2n+1)^2 P^2} \qquad \ldots(2.71)$$

and the radial component of the flux density is given by

$$B_\theta = 2F \times \sum_{n=0}^{\infty} \frac{\dfrac{\text{Sin}(2n+1)\frac{\beta}{2} \text{Cos } (2n+1)P(\theta + \frac{\beta}{2})}{\beta (2n+1)P}}{(R_1 \text{Sin}\theta)^2 + (x_1 - m + R_1 \text{Cos } \theta)^2} \times$$

$$\text{Cos } (2n+1)P \left[\text{Tan}^{-1} \frac{m \text{ Sin } \theta}{R_1 + x_1 \text{Cos } \theta}\right] \qquad \ldots(2.72)$$

3.3. The space wave distribution is of the form

$M \cos P\theta$.

The radial component of flux density is given by equation (3.01) by putting $n = 0$ and replacing dM/π by M_0, we have

$$B_0 = F' \times \frac{\cos P\left[\tan^{-1}\frac{\alpha \sin\theta}{R_1 + R_2\cos\theta}\right]}{(R_1\sin\theta)^2 + (R_2 - \alpha + R_1\cos\theta)^2} \qquad \ldots(3.03)$$

where

$$F' = \frac{4\pi M_0}{K_1} \times \frac{1}{\left[\frac{K_1}{K_0}\right]^P - \left[\frac{K_1}{K_0}\right]^{-P}} \qquad \ldots(3.04)$$

3.0. ILLUSTRATIVE EXAMPLE

In this section, detailed calculations are shown to illustrate the method discussed earlier. A 3 H.P., 400 Volt, 3 Phase, 50 c/s, Cage induction motor is selected with the following parameters.

Number of pole pairs 'P' = 2

S_{FL}	= 3%	R_0	= 0.075 Ω
L'	= 0.08 Ω	R_1	= 0.0743 Ω
d	= 0.30 δ	δ	= 0.00043 Ω
	= 0.00009 Ω	K_c	= 0.95
B_0	= 0.40 Wb/m^2	γ	= 50 c/s

Ampere turns distribution at the stator surface is assumed to be of the form $M e^{jP\theta}$

The constants C and D can be evaluated by Equation (2.19) and (2.20) by putting n = 0 and replacing $4M/\pi$ by M . From equation 2.18, we have

$$C = D R_1^{-2P}$$

$$\text{or} \quad D = C \times 30.8 \times 10^{-6} \qquad \ldots(2.75)$$

Also from Equation (2.21) , we have

$$B_o = \mu_o \left[C R_o^{P-1} + D R_o^{-P-1} \right]$$

$$\text{or} \quad 4\pi \times 10^{-7} \left[C \times 0.75 + D (0.75)^{-3} \right] = 0.40 \qquad \ldots(2.76)$$

Simplification of Equation (2.75) and (2.76) gives

$$C = 24.8 \times 10^3$$

$$D = 76.3$$

Also

$$C R_o^{P-1} - D R_o^{-P-1} = \frac{MP}{R_o}$$

On putting the values of constant C and D . In the above expression, we get .

$$MP/R_o = 7000 \quad \text{i.e.} \quad M = 262$$

From Equations No. (2.28) , (2.29) , (2.30), (2.36) and (2.38) , we have

$x_1 = 1.379$ $\qquad$ $x_2 = 1.380$

$m = 1.37$ $\qquad$ $K_1 = 36.9$

$K_2 = 38.7$ $\qquad$ $F' = 1.11 \times 10^{-3}$

$$B_\theta = 1.11 \times 10^{-3} \frac{\text{Cos } 2\left[\text{Tan}^{-1} \frac{1.37 \text{ Sin } \theta}{0.0745 + 1.379 \text{Cos} \theta}\right]}{0.018\ (\ 1.379 + 0.0745 \text{ Cos } \theta)}$$

The values of B_θ have been determined correct to three significant figures and are given in Table 1. The values of B_θ are plotted against θ in Fig. 2.4. The curve evidently contains both even and odd harmonics.

Table 1

θ (In Deg.)	B_θ
0	0.0422
15	0.0370
30	0.0238
45	0.00344
60	-0.0182
75	-0.0356
90	-0.044
105	-0.041
120	-0.0266
135	-0.00337
150	0.0224
165	0.040
180	0.047
195	0.040
210	0.0224
225	-0.00337
240	-0.0265
255	-0.0412
270	-0.044
285	-0.0356
300	-0.0182
315	0.00344
330	0.0238
345	0.0370
360	0.0422

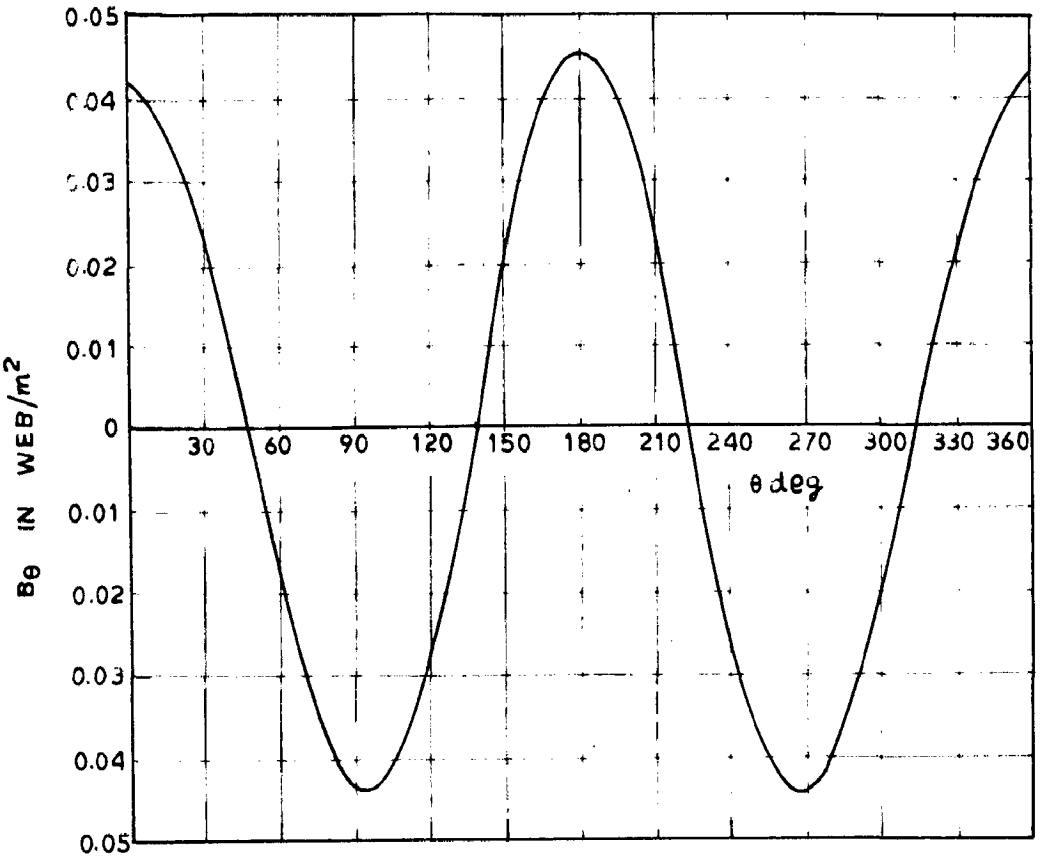

FIG. 2.4. RADIAL COMPONENT OF MAGNETIC INDUCTION AT THE SURFACE OF AN ECCENTRIC ROTOR

$\theta = 0^\circ$ MAXIMUM AIR GAP

$\theta = 180^\circ$ MINIMUM AIR GAP

C H A P T E R - 3

CALCULATION OF UNBALANCED PULL DUE TO ECCENTRIC ROTOR AND ITS EFFECT ON CRITICAL SPEED

3.1. CALCULATION OF UNBALANCED PULL

An unbalanced pull may be defined as the net side ways force between the stator and the rotor of an electrical machine resulting from a difference in the air-gap flux densities on the opposite side of the machine. The magnetic pull in Newton/ Meter square resulting from Maxwell's tensile stresses which occurs on the upper surfaces of stator and rotor is given by the formula

$$P = \frac{B^2}{2\mu_0} \quad \text{Newton/ meter}^2 \qquad \ldots(3.1)$$

The expression derived for the radial component of the flux density in Chapter 2 by rigrous method, may be used to calculate the unbalanced Magnetic pull (U.M.P) experienced by a non-salient pole machine with an eccentric rotor with the folloving assumptions :

1. Saturation is neglected.
2. Effects of slots and ventilating ducts are also omitted i.e., the air-gap of a machine is smooth and unslotted.
3. The permeability of rotor and stator material are assumed to be infinite.

The permeance in the eccentric air-gap (Fig. 3.1) may be represented by the equation of the form:

$$P' = P_0 + P_1 \cos\theta \qquad \ldots(3.2)$$

Where $\Theta = 0$, correspond to the maximum air-gap

$\Theta = \pi$, correspond to the minimum air-gap

Neglecting the Harmonics, the total air-gap m.m.f. can be expressed in the form :

$$a = M' \cos (P\Theta - wt) \qquad \ldots(3.3)$$

Multiplying equation No. (3.2) and (3.3) , we get the net air-gap field as :

$$B_g = (P_o + P_1 \cos \Theta) M' \cos (P\Theta - wt)$$

$$B_g = P M' \cos (P\Theta - wt) + \frac{P_1 M'}{2} \left\{ \cos \left[(P+1)\Theta - wt\right] + \cos \left[(P-1)\Theta - wt\right] \right\}$$

The radial magnetic force along a single stator radius is proportional to the square of the flux - density.

$$B_g^2 = \frac{P^2 M'^2}{2} \left[1 + \cos 2 (P\Theta - wt)\right] + \frac{P_o P_1 M'^2}{2} \left\{ \cos \left[(2P+1)\Theta - 2wt\right] + 2\cos\Theta + \cos \left[(2P-1)\Theta - 2wt\right] \right\}$$

$$+ \frac{P_1^2 M'^2}{8} \left\{ 2 + \cos 2 \left[(P+1)\Theta - wt\right] + \cos 2 \left[(P-1)\Theta - wt\right] + 2\cos \left[2P\Theta - 2wt\right] + 2 \cos 2\Theta \right\}$$

$\therefore$ The resultant force on the stator (or rotor) which is obtained by integrating the projection of the radial force component along a fixed axis is given by :

$$F_1 = \frac{DL}{4\mu_o} \int_0^{2\pi} B_g^2 \cos\Theta \, d\Theta \qquad \ldots(3.4)$$

After putting the value of B_g in the above expression and integrating it within the proper limits, we get

$$F_1 = \frac{DL}{4\mu_o} P_o P_1 M'^2 \pi \qquad ..(3.5)$$

The value of the constants P_o and P_1 can be calculated with the help of equations (2.73) and (3.1). Thus we have,

$$\left.\begin{aligned} P_o + P_1 &= \frac{B_{max}}{M'} \\ P_o - P_1 &= \frac{B_{min}}{M'} \end{aligned}\right\} \qquad ...(3.6)$$

The minimum and maximum value of the flux density is calculated by Equation No. (2.73) by putting $\theta = 0$ and $\theta = \pi$ respectively.

$$\left.\begin{aligned} B_{min} &= \frac{F}{A\,(x + R_1)} \\ B_{max} &= \frac{F}{A(x - R_1)} \end{aligned}\right\} \qquad ...(3.7)$$

Where $$F = \frac{4\mu_o\, m\, M\, P}{K_1} \cdot \frac{1}{\left|\frac{K_1}{K_2}\right|^{P} - \left|\frac{K_1}{K_2}\right|^{-P}} \qquad ...(3.8)$$

and $$A = 2\,(x_1 - m) \qquad ...(3.9)$$

From Equation No. (3.6) and (3.7), we get

$$P_o = \frac{F x_1}{2M'(x_1 - m)(x_1^2 - R_1^2)} \qquad ...(3.10)$$

$$P_1 = \frac{P\left(n_1^2 - n_0^2 - n_2\right)}{2\pi'\left(n_2 - n\right)\left(n_1^2 - n_0^2\right)} \qquad \ldots (3.11)$$

After having the values of constants P_0 and P_2, the U.M.P. experienced by a corresponding pole-machine with concentric rotor can be calculated by equation No. (3.3).

3.2. GRAPHICAL METHOD OF CALCULATION OF UNBALANCED PULL TAKING INTO ACCOUNT THE EFFECT OF SALIENCY AND SATURATION

3.2.1. MULTIPOLAR SALIENT POLE MACHINES

The stator and the rotor are assumed to have smooth cylindrical iron surfaces with the centres displaced by an amount ϵ (eccentricity). Without displacement the radial air gap would have a constant value δ. The diameter drawn through the two centres has been defined as 'symmetry diameter'. The exciting coils are assumed to give sine number of sinusoidal. Owing to the eccentricity the air-gap at one place in the symmetry diameter will reduce to $\delta - \epsilon$, in the opposite place increased to $\delta + \epsilon$. At any point the radius through which describes an angle θ with the symmetry diameter, the change in the air-gap can be expressed as $\epsilon \cos\theta$ approximately. At right angles to the symmetry diameter the increase or reduction in the air-gap will be practically zero.

The flux emitted by one field pole returns through the contiguos halves of the neighbouring poles. In a bipolar machine the flux of each pole is same inspite of air-gap differences. In multipolar machine the poles of one half of the machine will carry a greater flux then those of the other half, unless the winding arrangement prevents it - (equalizing connection). Apart from this the flux in each pole will be different from that of the others, dependent upon the local air-gap. Poles in the diameter at right angles to the symmetry diameter will carry the normal flux, for their neighbouring poles in the one half (with reduced air-gap) will tend to increase their flux just as much as those in the other half (with increased air-gap). The result is that in a multipolar machine, each pole should be considered as it it would create its own flux and not be dependent upon adjacent poles.

Let us assume that the machine be excited to give with mean air-gap, a flux density of B web/meter^2 of the pole face and also let.

B_2 = Flux density corresponding to the reduced air-gap $\delta - \epsilon$

B_1 = Flux density corresponding to the increased air-gap $\delta + \epsilon$

Since $B_2 > B_1$, the flux density B_2 gives the greater magnetic pull in one direction than the flux density B_1, in the opposite direction and the

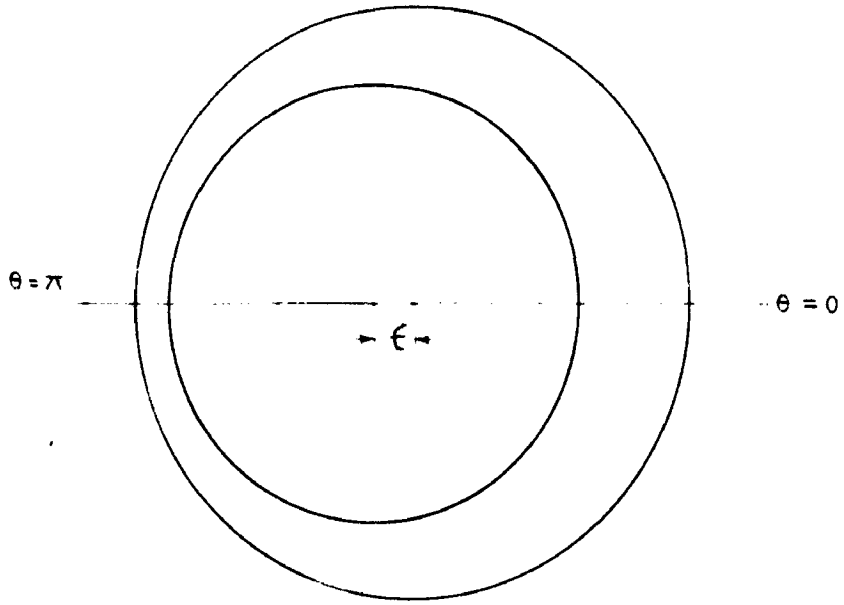

FIG. 3.1

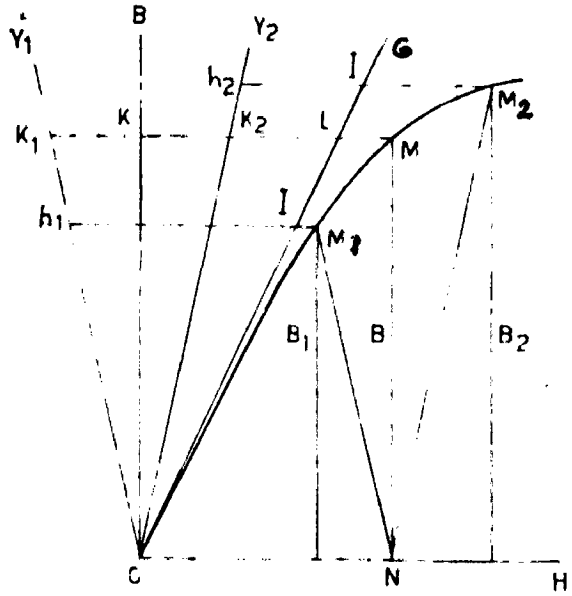

FIG 3.2

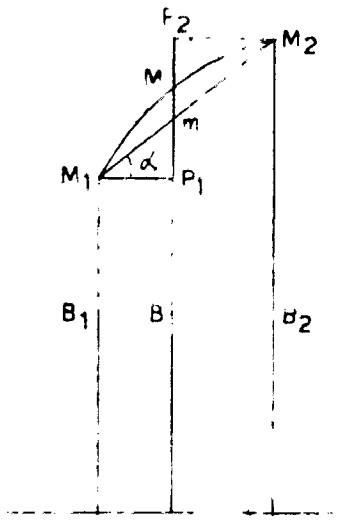

FIG. 3.3

CALCULATION OF FLUX DENSITIES B1 AND B2 FROM MAGNETIZATION CURVE

difference of the two pulls or the 'local unbalanced pull' in Newton/ Meter^2 of the pole surface is given by the formula

$$p = \frac{(B_2^2 - B_1^2)}{2\mu_0} = \frac{(B_2 - B_1)(B_2 + B_1)}{2\mu_0} \quad \ldots (3.33)$$

B_2 and B_1 can be easily determined if the magnetic characteristic of the machine is given. In Fig. 3.3, the abscissa represents the exciting m.m.f. per pole, while the ordinate B represents the flux density per meter square of the pole face with the normal air-gap.

ON = K1, represents the m.m.f required to produce the induction B.

OG is the air-gap line.

KL = M.M.F. required for the magnetisation of the air-gap.

LM = M.M.F. required for the magnetisation of the iron.

The flux densities B_1 and B_2 can be calculated by drawing through 'O' two lines OY_1 and OY_2 such that for any induction B = (N1), K_1L represents the m.m.f. required for the air-gap $G = 1$ and K_2L represents the m.m.f. required for the air-gap $G = 2$. We then draw two lines through N parallel to OY_1 and OY_2. These lines intersect the magnetisation curve at M_1 and M_2, which give the actual air-gap flux density B_1 and B_2 under the poles with the increased and reduced air-gap for a given excitation ON. Because

$$B_1 M_1 = B_2 M_2 = ON$$

In general, the abcissas of the lines OY_1 and OY_2 (Fig. 3.2) will bear to the abcissa of OG for the same flux density very nearly the ratio of the displacement δ to nominal air-gap . But if the displacement is very greate compared with the average air-gap and if the machine has open slots, the proportionality will be disturbed due to the crowding of the flux lines in the air- gap near the teeth. For small displacement OY_1 and OY_2 can always be drawn symmetrical with reference to the ordinate and the m.m.f. for the given induction B is approximately $\pm \delta B / \mu_o$, where displacement is measured in meters.

In Fig. 3.3, the part M_1M_2 of Fig. 3.2. is drawn on the greater scale and also the chord M_1M_2 which cuts the ordinate of point M in m . The chord describes with the horizontal an angle α .

$$P_1P_2 = P_1m + P_2m = (M_1P_1 + M_2P_2) \text{Tan } \alpha$$

M_1P_1 and M_2P_2 are the abcissas of the δ characteristics for inductions B_1 and B_2 respectively, and are therefore equal to $\delta B_1 / \mu_o$ and $\delta B_2 / \mu_o$.
Therefore we have :

$$P_1P_2 = B_2 - B_1 = \frac{(B_2 + B_1) \delta \text{ Tan } \alpha}{\mu_o} \qquad ..(3.13)$$

∴ From equations No. (3.12) and (3.13), we have,

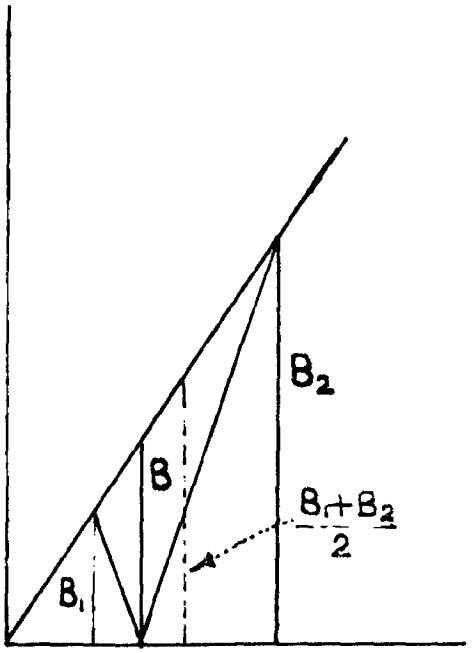

FIG 3·4

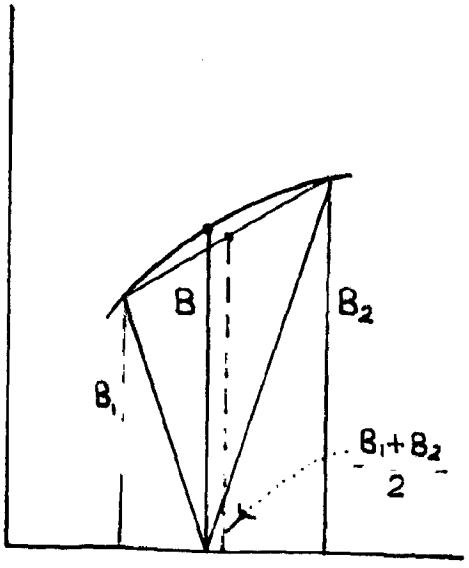

FIG 3·5

$$p = \frac{(B_2 + B_1)^2 \alpha \text{ Tan } \alpha}{2 \mu_0^2} \qquad \ldots\ldots (3.16)$$

If α is not very great, the sum $(B_2 + B_1)$ can accurately be replaced by $2B$, and the angle which the chord forms with the horizontal can be replaced by the angle formed by the tangents at the point M with the horizontal. Tan α is then the gradient of the curve at point M and can be expressed as a differential quotient dB/dH.

∴ The unbalanced magnetic pull in Newton/ meter^2 is, therefore

$$p = \frac{4 B^2}{2 \mu_0^2} \alpha \frac{dB}{dH}$$

$$p = 2 \left(\frac{B}{\mu_0}\right)^2 \alpha \frac{dB}{dH} \qquad \ldots (3.17)$$

If α is large and if the magnetisation characteristic were a straight line (Fig. 3.4), the sum $B_2 + B_1$ would actually be greater than $2B$. The value of $B_2 + B_1 / 2$ is shown dotted in Fig. 3.4. If however, the characteristic is strongly curved (Fig. 3.3), $B_2 + B_1$ will be slightly smaller than $2B$. For hard pulling over, when α reaches the greatest possible value, the saturation in that case will be high enough that the curvature of the characteristic is marked. It is therefore certain that the formula (3.9) does not give too low values for the extreme case.

3.2.2. EFFECT OF EXCITATION ON UNBALANCED PULL

The first part of almost every magnetization curve is a straight line going through the origin of the coordinates. For every straight line characteristic, the gradient dB/ dH is constant, the U.M.P. will grow therefore with the square of the induction B. But as soon as the saturation of the iron part is noticeable, the quotient dB/dH will constantly diminish. The problem now is to find the induction B for which the product $B^2 \frac{dB}{dH}$ is a maximum. This, in fact, can be calculated by graphical method explained in Fig. 3.6.

For a point M of the saturation curve I , the ordinate B = NM is drawn and a line MP perpendicular to the direction of the curve in point M. The angle NMP is identical with the angle α formed between the curve in point M and the horizontal. We have,

$$\text{Tan } \alpha = \frac{dB}{dH} \quad \text{and} \quad NP = NM \text{ Tan } \alpha = B \text{ Tan } \alpha$$

$$\therefore \text{ Area of the triangle NMP } = \frac{1}{2} \cdot B.B. \text{ Tan } \alpha = \frac{B^2}{2} \frac{dB}{dH}$$

If such triangles are drawn for different points of the curve, the triangle area will be proportional to $B^2 \frac{dB}{dH}$ for the various points.

In order to obtain a curve representing the magnetic pull for every excitation, it is now only necessary to replace all the triangles NPM by others which have a

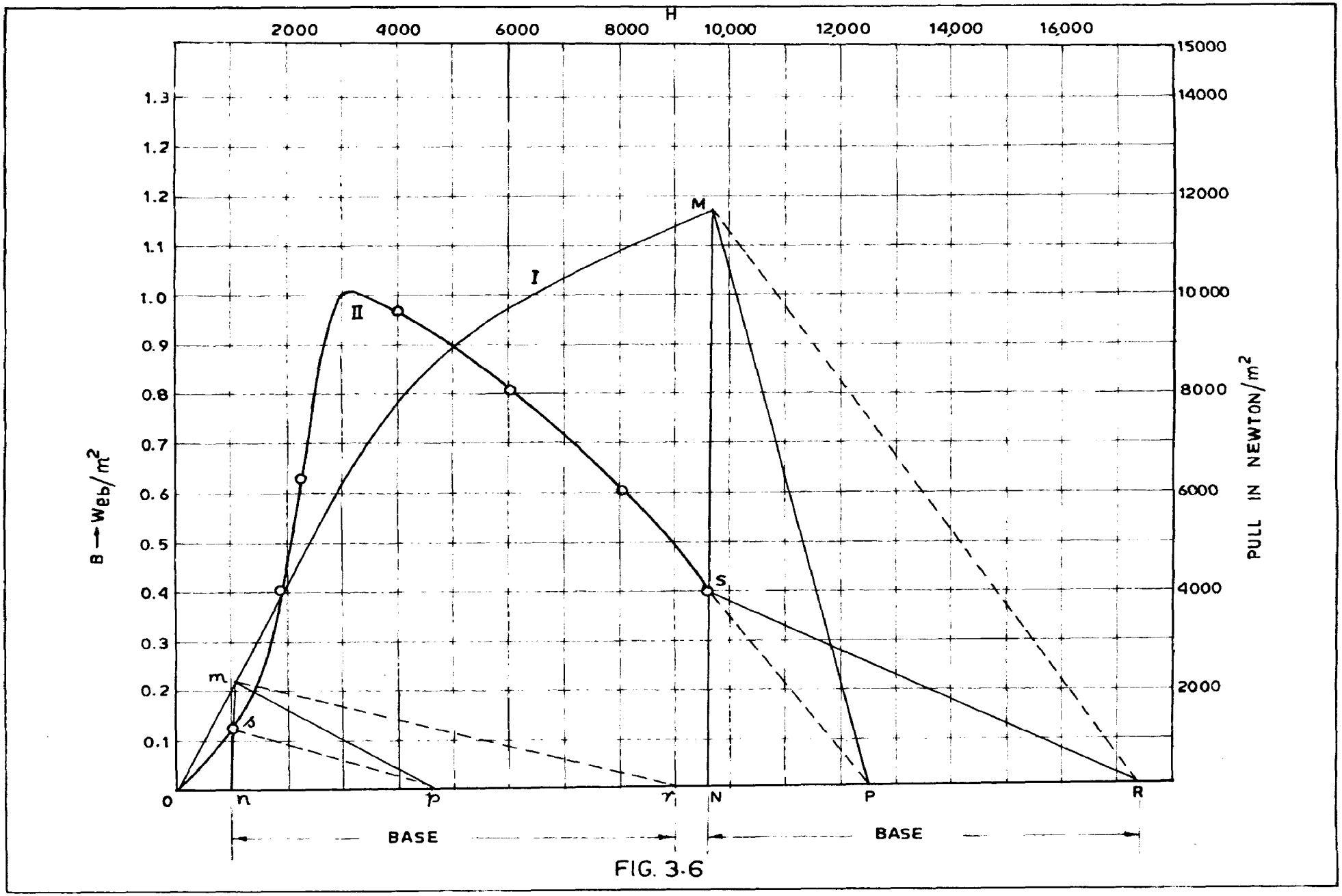
H
2000
4000
6000
8000
10,000
12,000
14,000
16,000
15000
14000
12000
10 000
8000
6000
4000
2000
PULL IN NEWTON/m²
B → Web/m²
1.3
1.2
1.2
1.1
1.0
0.9
0.8
0.7
0.6
0.5
0.4
0.3
0.2
0.1
M
I
II
S
m
s
0
n
p
r
N
P
R
BASE
BASE

FIG. 3·6

suitable ordinary base NR. Connecting R with M and drawing a line PS parallel to NI , it follows from the elementary geometry that the triangles NPI and NRS are equal in area. NS is therefore a measure of the function $B^2 \frac{dB}{dM}$. The scale is determined by the base NR. If the construction is repeated point for point, we get a bold line curve II in Fig. 3.6. The first part of which corresponding to the straight portions of the magnetisation characteristic, consists of a parabola with vertical axis, but as the magnetisation characteristic begins to bend, the curve of the pull reaches its maximum and from then falls steadily.

Until now we have calculated the U.M.P. per square meter for an eccentricity ϵ . The eccentricity changes in a quadrant from ϵ to zero according to the expression $\epsilon \cos\theta$. The U.M.P. in different parts of a multipolar machine will therefore be very nearly proportional to $\epsilon \cos\theta$ and the component of this pull working along the 'symmetry direction' will be proportional to $\epsilon \cos\theta$. $\cos\theta = \epsilon \cos^2\theta$. In machines with a number of poles divisible by 4 , we may always consider together two points, separated by a full quadrant with an angle θ , the other with angle $(\alpha + \theta)$. The sum of the components of these pulls / meter^2 is -

$$p = 2\left(\frac{B}{\mu_0}\right)^2 \frac{dB}{dl}\left[\left(\epsilon \cos^2\theta + \epsilon \cos^2(\alpha+\theta)\right)\right]$$

$$D = 2 \left(\frac{B}{\mu_0}\right)^2 \frac{dB}{dH} \delta$$

In such a machine, we can therefore always find two pole pairs which, taken together, develop the same unbalanced pull as a single pole of identical dimensions and induction , the axis of which is parallel and the pole face of which is perpendicular to the symmetry diameter.

In a six pole machine, three pole pairs together develops 3/2 times the unbalanced pull of an imaginary pole pairs with an axis parallel and a pole face perpendicular to the symmetry diameter. The same investigation for 10 , 14 poles would confirm that

> ' The total U.M.P. can be calculated in all multipolar machines, as if the air-gap were reduced by an amount δ in one quarter of all the poles and increased by δ in another quarter of all the poles, and left alone in the remaining two quarters. '

The total U.M.P. 'F' of the whole machine will therefore be obtained, if we multiply equation No. (3.13) with one quarter of the total pole face area of the machine.

$$F_1 = \frac{PA}{8} 2 \left(\frac{B}{\mu_0}\right)^2 \delta \frac{dB}{dH}$$

$$F_1 = PA \left(\frac{B}{\mu_o}\right)^2 \prec \frac{dB}{dH} \qquad \ldots(3.16)$$

Let B_m be the induction at the end of the straight line characteristic which gives the same magnetic pull as is actually obtained by the critical induction (at which U.M.P. is maximum) In reality B_m will be slightly less than the critical induction, but with small inaccuracy we can assume B_m as critical induction. For the straight line part of the characteristic going through the origin, we can replace

$$\frac{1}{\mu_o} \prec \frac{dB}{dH} \text{ by } \frac{\prec B}{\mu_o H} \text{ or } \frac{T_\prec}{T_c}$$

Where $T_\prec$ represents the ampere turns required to produce in an air-gap $\prec$ any flux density with the unsaturated region and T_c represents the ampere turns per pole, required to produce the magnetic circuit of the machine with the correct air-gap for the same flux density.

The equation (3.16) takes the simple form :

$$F_1 = \frac{P A B^2}{\mu_o} \frac{T_\prec}{T_c} \qquad ..(3.17)$$

or $$F_1 = \frac{P A B^2}{\mu_o} \frac{\prec}{\delta_1} \qquad ..(3.18)$$

Where δ_1 = virtual air-gap which would take, for an induction within the straight line characteristic as many ampere turns as the real air-gap and the iron path of the magnetic half circuit together.

For machines with smaller air-gap , as in Induction motor, the virtual air-gap is appreciably higher than the real air-gap, say 30 percent higher or more, while in generators, especially turbogenerators, the virtual air-gap is nearly equal to the actual one.

Instead of total pole face area 2 PA, we can substitute the cylindrical field surface C π DL where C represents the pole factor (Pole arc/Pole pitch).

$$\therefore F_1 = \frac{1}{2} \quad \frac{C \pi DL \; B^2}{\mu_o} \quad \frac{\lambda}{\delta_1} \qquad \ldots (3.19)$$

3.2.3. BIPOLAR SALIENT POLE MACHINE

In a multipolar machines the flux leaving the field at a place where the air-gap is reduced by the eccentricity, also returns into the field where the air-gap is reduced. The sum of all the fluxes taken over one half of the machine will therefore be greater than the sum of all the fluxes taken over the other half of the machine.

(a) DISPLACEMENT OF ROTOR AT RIGHT ANGLE TO THE FIELD AXIS

The same possibility exists in a two pole machine, if the eccentric displacement is at right angles to the field axis as shown in Fig. (3.7).

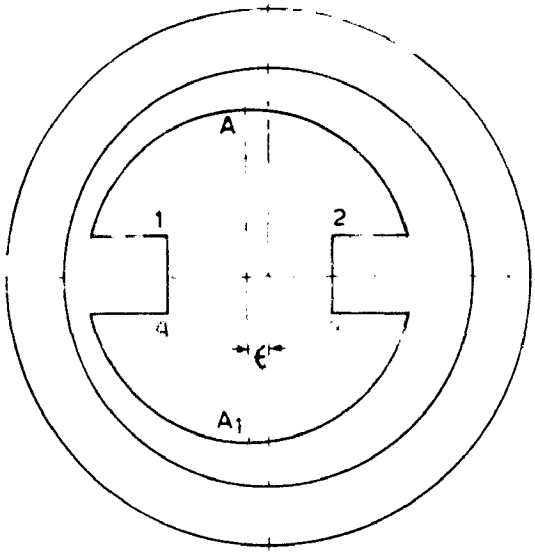

FIG.3.7 DISPLACEMENT OF ROTOR AT RIGHT ANGLE TO THE FIELD AXIS

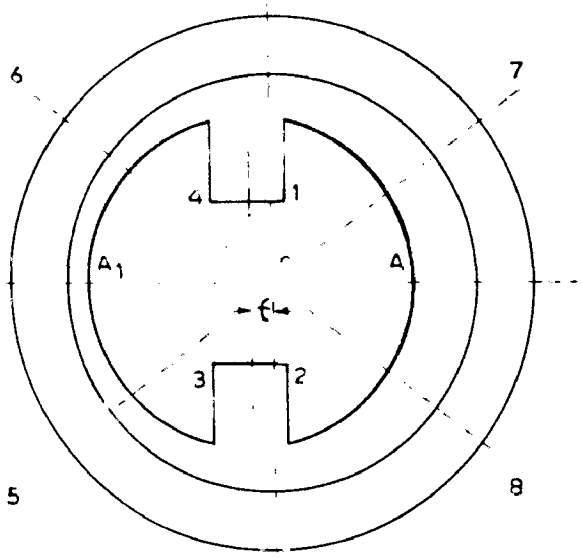

FIG 3.8 DISPLACEMENT OF ROTOR IN THE DIRECTION OF FIELD AXIS

A motor is operated with salient poles having one exciting coil. The field coils AA_1 has a distance d from the stator centre. The flux paths are shown in Fig. 3.7. In the half machine on the left side of the coils AA_1, the air gap is throughout smaller than on the right side, and so the two sides represent two parallel magnetic paths with different reluctances, the total flux on the left side will be greater than the total flux on the other side.

This case is similar to that of a multipolar machine except for the fact that through the armature there is considerable amount of unbalanced pull in one-one, while the saturation of the stator and rotor core is highly influenced by the unequal distribution of the fluxes in the two machine parts. In order to find the air-gap flux densities B_2 and B_3 corresponding to certain displacement δ, a magnetic characteristic of the air-gap, tooth and pole tips should be drawn including the exciting curve required for the core, and therefore the critical induction B_n will be higher and the local unbalanced pull will be greater than it would be if the magnetic characteristic of the whole machine had to be considered.

(b) DISPLACEMENT OF ROTOR IN THE DIRECTION OF FIELD AXIS

A different effect of eccentric rotor is to be displaced with respect to stator centre

by an amount ϵ in the direction of the field axis (Fig. 3.8). Although the air gap in the left half is smaller than in the right half, the total flux must be equal in both halves, if no flux can return through the neutral zone. The flux passes in series through the smaller and the larger air-gaps. The only effect of eccentricity will be different distribution of the flux over the pole faces.

Let us assume for simplicity sake that the rotor in a central position, the air-gap induction over the whole pole face would be equal. Then it is evident from Fig. (3.8), the flux density will be minimum in the centre A of the right pole, where the air-gap is maximum, while it will increase gradually to the corner 1 and 2 of the right pole. In the left pole, however, the flux density will be maximum in the pole centre A_1 and will grade down towards the corner 3 and 4 . Therefore an unbalanced pull will act directed towards left.

Within the portion 5-0-6 shown in Fig. 3.8, the flux density will be greater, and in the corners 3 and 4 smaller than the average. In the opposite portion 7-0-8, the flux density will be smaller and in the corners parts 1 and 2 greater than the average. The portions mentioned will contribute an unbalanced pull directed to the left, the corners parts a smaller component directed to the right. It

is clear that total U.M.P. is smaller than in Fig. 3.7. A two pole rotating field, therefore, experience on U.M.P. which changes twice during a revolution from a maximum to minimum value.

In practice a salient pole of two pole machine covers about 120°. In the case corresponding to Fig. 3.7, the limits of θ from 1 to A are $\pi/6$ to $\pi/2$. An element of the surface covering an infinitely small angle $d\theta$ has an area $1/2\ DL d\theta$ component of U.M.P. in a horizontal direction contributed by the element is

$$= \frac{1}{2} DL \cdot 4 \frac{B^2}{2\mu_o} \cdot \frac{\delta}{\mu_o} \cdot \frac{dB}{dH} \cos^2\theta$$

The integration must be made from $+30^{\circ}$ to $+90^{\circ}$ and from -30° to -90° or the integration made from 30° to 90° must be doubled.

$$F_1 = \frac{DL \cdot 4B^2}{2\ \mu_o} \cdot \delta \frac{dB}{dH} \int_{\pi/6}^{\pi/2} \cos^2\theta$$

$$= 1.228\ DL \frac{B^2}{2\mu_o} \cdot \frac{\delta}{\delta_i}$$

$$F_1 = 0.39\ \pi\ DL \frac{B^2}{2\mu_o} \cdot \frac{\delta}{\delta_i} \text{ Newtons} \qquad \ldots(3.20)$$

The pole factor is 0.39 instead of accustomed value of 2/3 comparing equations No. (3.19) and (3.20) we see that the unbalanced pull in case of two pole salient pole machine with 120° pole angle is only 59% of that of multipolar machine of same dimensions and total pole area, provided that the critical induction and virtual air-gap are same in both the cases.

3.3. INCREASE OF ECCENTRICITY DUE TO UNBALANCED PULL

A displacement of rotor from its true central position causes a one sided magnetic pull. A one sided magnetic pull, on the other hand, causes a further displacement. There is a force working on the stator and the rotor pulling them towards each other in the direction where the air-gap is a minimum. This will cause not only an elastic deflection of roter shaft but also of the stator frame, of the bed plate and of the pedestals. If the machine is not excited, all its parts experience a certain deflection due to the weights. The elastic deflections of all parts will change if a one sided magnetic pull occurs, whatever its direction may be . A magnetic pull directed upward will reduce the apparent weight of the rotor and increase the apparent weight of stator. The transfer of this weight from the rotor bearing to the feet of the stator frame will also change the elastic defelction of the bedplate. The absolute value of the difference will be same, whether the unbalanced pull on the rotor is directed upwards or downwards.

From equation No. (.3.19) , the U.M.P. is proportional to the displacement ϵ . The elastic deflections of all the machine parts caused under the influence of 'F_1' are proportional to this force, therefore, also proportional to the initial displacement ϵ . The

sum of these deflections constitute the 'first increment' of the original displacement. This increment in displacement will cause an increment in one sided magnetic pull which bears the same ratio to the original pull as the increment in displacement bears to the original displacement. The increment in pull would cause a second increment in displacement, the second increment in pull would cause a third increment in displacement. As long as the proportionality between displacement and pull exists, every following increment will have the same ratio to its immediate predecessor as this to its own predecessor . The initial displacement and its increments are represented by a geometric series, which can be e-xpressed in the form:-

$$\alpha + q\alpha + q^2\alpha + q^3\alpha + \ldots\ldots$$

The sum of this series is finite value, if $q\alpha$ is smaller than α i.e., q is less than unity.

$\therefore$ Final static displacement is given by $\alpha' = \frac{\alpha}{1 - q}$ ...(3.21).

On substituting α' instead of α in the previous formulae, the Final static force of the unbalanced pull is known.

EFFECT OF EXCITATION

If the machine is suddenly excited, as it is generally the case with an induction motor, the shaft

frame and other parts of the machine will not only deflect so as to increase the initial displacement α to final displacement α', but all parts of the machine being elastic will overshoot the position of new static equilibrium like a spring or a chord. The distance travelled by the parts of the machine from old position to the new is $\alpha' - \alpha$ and they will over-shoot this position by approximately the same amount. The momentary displacement therefore will be

$$\alpha_{mom} = \alpha + 2(\alpha' - \alpha) = 2\alpha' - \alpha$$

$$= \alpha \frac{1 - q}{1 + q} \qquad \ldots\ldots (3.22)$$

Therefore the original mechanical displacement must be multiplied by $\frac{1 - q}{1 + q}$ to obtain the displacement occurring at the moment of switching in.

We can now formulate the requirement, that a machine, say induction machine, should be free from 'pulling over', even if the initial displacement of the retor is equal to one half of the mean airgap. In other words the displacement at the moment of switching in, should be less than twice the initial displacement.

$$\text{i.e.,} \quad \frac{1 + q}{1 - q} < 2$$

$$\text{or} \quad q < 1/3$$

The smaller the q, the safer is the machine against pulling over.

3.4. INFLUENCE OF UNBALANCED PULL ON CRITICAL SPEED

If the centre of gravity of rotor does not coincide with the axis of rotation, but has a distance α from the same, a centrifugal force will be developed which is proportional to the displacement α and to the square of the number of revolution per minute. At certain speed the centrifugal force will be so great that it would cause (in the absence of friction etc.,) a deflection of the shaft equal to the original displacement. The displacement being doubled, the centrifugal force will be doubled causing a double increment in deflection etc., At this speed so called 'critical speed' an original displacement, if not infinitesimal, would cause an infinite final displacement, if there were no resistance to the movements. Although in reality, the resistance will keep the displacement down to the finite values. The great increase of vibration at the critical speed is highly objectionable and there is always careful calculation in the design of high speed machines to make sure that the running speed is well above or well below the critical speed :

Let α = displacement in cms ,

W = weight of rotor in Kilograms

f = Gravity deflection in cms, caused under the static influence of rotor weight w.

Then the centrifugal force

$$= 4 \frac{W}{9.81} \frac{\alpha}{100} r^2 \left(\frac{N}{60}\right)^2 = \alpha \; W \left(\frac{N}{300}\right)^2 \qquad \ldots (3.23)$$

Let q_r the ratio of the roter defelction caused by the unbalanced pull to the displacement causing the unbalanced pull. Then the force of unbalanced pull caused by deflection f is

$$F_f = q_r W \qquad \ldots(3.24)$$

But if the stationary parts of the machine are assumed to be infinitely stiff, then $q_r = q$ and the U.M.P. for a displacement α is given by

$$\frac{\alpha}{f} q W \qquad \ldots(3.25)$$

∴ The sum of the centrifugal force and unbalanced pull is

$$P = \alpha W \left(\frac{N}{300}\right)^2 + \frac{\alpha}{f} q W \qquad \ldots(3.26)$$

The elastic gravity defection, caused by the weight W is f , so the elastic deflection caused by one Kilogram is f / W . The elastic deflection caused by the force P is given by multiplying equation №. (3.26) by f / W , which gives

$$\frac{f}{W}\left[\alpha W \left(\frac{N}{300}\right)^2 + \frac{\alpha}{f} q W\right] = \alpha\left[f \left(\frac{N}{300}\right)^2 + q\right]$$

For the critical speed this deflection should be equal to the original displacement α . The expression in the bracket therefore will be unity for critical speed N

$$f \left(\frac{N_c}{300}\right)^2 + q = 1$$

$$\therefore N_c = \sqrt{1 - q} \; \frac{300}{\sqrt{f}} \qquad \ldots(3.27)$$

For unexcited machine, $q = 0$, and the critical speed is given by :-

$$N_c = \frac{300}{\sqrt{f}} \qquad \ldots\ldots(3.29)$$

The critical speed is reduced, if the machine becomes excited and will be lowest for that excitation which given the highest value of unbalanced pull.

3.5. ILLUSTRATIVE EXAMPLE

3.5.1. CALCULATION OF U.M.P. BY RIGROUS METHOD

Let us consider an Induction motor of 5 H.P., 400 volt Δ connected, 1500 r.p.m.

The various calculated parameters of the machine in question is given below :

P	= 2	m_1	= 3
D	= 0.15 m	L	= 0.09 m
Np_1	= 96	Kb_1	= 0.955
Kp'_1	= 1	η	= 0.83
Cos ϕ	= 0.84		

I_1 = Primary current $= \dfrac{5 \times 0.746}{3 \times 400 \times 0.83 \times 0.84} = 4.5$ Amp.

Primary m.m.f. in ampere turns/pole is given by

$$A_1 = \frac{2\sqrt{2}}{\pi} Kb_1 Kp_1 m_1 Np_1 I_1 = N_1' I_1$$

$$\therefore \quad N_1' = \frac{2\sqrt{2}}{\pi} \times 0.955 \times 3 \times 96 = 247$$

No load current I_o = 3.5 ampere.

Net air-gap ampere turns/ pole = $I_o N_1'$

= 3.5 x 247 = 865

∴ Total Net air-gap ampere turns = M' = 4 x 865 = 3460

$$U.M.P. = \frac{DL}{4\mu_o} P_o P_1 M'^2 \pi$$

$$P_o = \frac{F x_1}{2M' (x_1 - m) (x_1^2 - R_1^2)}$$

$$P_1 = \frac{F (x_1^2 - R_1^2 - x_1)}{2 M' (x_1 - m)(x_1^2 - R_1^2)}$$

The values of F , M , x_1 , m has been calculated in Section 3.6 of Chapter 3 for the same motor. On putting the value in the above expression we get ,

$P_o = 1.73 \times 10^{-4}$, $P_1 = 0.625 \times 10^{-4}$

$$F_1 = \frac{.075 \times .00 \times .625 \times 1.73 \times 10^{-8} \times (3460)^2}{2 \times 4\pi \times 10^{-7}}$$

F_1 = 1100 Newton.

U.M.P. = 1100 / 9.81 = 113 Kilogram.

3.5.2. CALCULATION OF U.M.P. BY GRAPHICAL METHOD TAKING INTO ACCOUNT THE EFFECT OF SATURATION - EXAMPLE 2.

Let us consider an alternator with number of poles = 40

Pole face Area = .0850 m^2

Radial air-gap = .0031 m

Critical Induction = 0.63 web/m^2, ℓ = .001 meter.

The Magnetic characteristic of the machine is shown in Fig. 3.6. The Curve II of Fig. (3.6) shows that the maximum U.M.P. is 100000 Newtons / meter^2 and it can be verified for any particular induction on the straight part of the magnetization characteristics. The straight part of the line goes through a point with an ordinate B = 0.43 web/m^2 and H = 2000

$$\therefore \text{ The ratio } \frac{\prec}{\mu_o} \frac{dB}{dH} = \frac{0.43 \prec}{2000 \times 4\pi \times 10^{-7}}$$

$$= 172 \prec$$

$$P = 2 \frac{B_m^2}{\mu_o} \frac{\prec}{\mu_o} \frac{dB}{dH}$$

$$= 2 \frac{(0.63)^2}{4\pi \times 10^{-7}} \quad 172 \quad \times .001$$

$$= 108000 \text{ Newton / m}^2$$

The method of calculation gives the result 8% higher than that of graphical method, which is entirely satisfactory.

U.M.P. of the whole machine can be calculated by Equation (3.16)

$$F_1 = PA \frac{B^2}{\mu_o} \frac{1}{\mu_o} \frac{\prec dB}{dH} = 70,000 \text{ Newtons.}$$

If we had used formula (3.18), instead of (3.16), we should have obtained at first from straight line characteristic virtual air - gap

$$= \frac{3000}{0.40} \times 0.7 \times 10^{-7} = 0.000 \times 10^{-3}$$

$$\therefore \quad P = \frac{\rho_1 D_1^3}{\delta_0} \cdot \frac{d}{\delta_1} = 70,000 \text{ Newton.}$$

3.3.3. PERMISSIBLE GRAVITY DEFLECTION :

The permissible gravity deflection can be calculated directly from equation No. (3.25). The characteristic of the machine is shown in Fig. (3.6). The rotor of which has a weight W = 0000 K.gms.

Suppose we want to allow U.M.P. of not more than say 1/0 th of the rotor weight i.e. 1500 K.g. for a displacement equal to gravity deflection.

But the U.M.P. for .001 m displacement is 70,000 Newtons.

$$\therefore \text{ Permissible gravity deflection } \delta = \frac{1500 \times 0.01}{70,000} \times .001$$

$$= .0021 \text{ m.}$$

Therefore the shaft must be made strong enough so that this deflection is not exceeded.

3.3.4. INFLUENCE OF U.M.P. ON CRITICAL SPEED

To illustrate the influence of the U.M.P. on the critical speed, let us consider a 2 pole machine having the cylindrical surface equal to 1.01 m^2.

Actual radial air gap = .010 m

Virtual air gap = 0.010 m.

case rotor weight

Virtual air gap $= 0.003$ m

Radial air - gap $= 0.003$ m

Critical Induction $B_g = 0.3$ Wb/m^2

$$q = \frac{g}{0.3} \quad \frac{0.003 \times 1.31 \times (0.3)^2}{3000 \times 0.01 \times 3 \times 47 \times 10^{-7}} = 11.2\ g$$

$= 11.2 \times 0.007 = .078$ for 30 r.p.m.

$= 11.2 \times .278 = 0.31$ for 1800 r.p.m.

In the latter case the critical speed would be reduced by the magnetic pull

$$N_c = \sqrt{1 - 0.31} \times 1800 = 1800 \text{ r.p.m.}$$

This is not acceptable for a machine running at 1800 r.p.m.

8.0. CONCLUSIONS

1. From equation (3.3), we can find U.M.P. experienced by a non salient pole machines for eccentricity upto about $\delta = 0.30\ \delta$, which is normally considered to be maximum permissible in any practical machine. For larger eccentricities, however, the U.M.P. calculated by the above formula is bound to exceed the pull actually experienced by the machine. The reason being that under these conditions of operation, magnetic induction in the air-gap in and around the region of $\theta = 180^\circ$ would become very large, causing excessive saturation in the stator and

the rotor materials, which would in turn reduce the magnetic pull considerably as shown by graphical method.

But this objection is not of much importance as a rule. Since the object of calculating U.M.P. is chiefly to ascertain the reduction in the rigidity of the shaft and hence the magnitude of stress and deflection actually occurring within the limiting conditions $\delta = 0.20\,\delta$. The stress in the shaft and the load on the bearing when pull over occurs is no. of course, calculable from purely mechanical considerations.

Independently of these considerations any calculation of U.M.P. are subjected to error due to :

i. Magnetic saturation.

ii. Effects of parallel circuits in the armature winding, since such circulating currents tend to reduce the magnetic inequalities in the air-gap and hence also the U.M.P.

iii. and effects of slotting, a cylindrical machine with number of slots behaves in a very different way from an idealised machine in many aspects, including the effect of rotor eccentricity.

The air-gap flux plays a significant part in the development of unbalanced forces due to eccentricity and this component of leakage has not been represented in an adequate way in the analysis based on smooth cylindrical surfaces.

2. The effect of U.M.P. due to eccentricity may be of two fold character. If the outer rotor surface and the inner surface are truly cylindrical but not concentric, while the rotor taken itself is running true (i.e. static eccentricity), the forces occasioned by the unbalanced pull have always the same direction in space independent of the rotation and are in case of multipolar machines constant, and only in case of two pole rotating fields variable.

If, however, the rotor taken itself is untrue (i.e. Dynamic eccentricity), no matter whether the field or armature is rotating, then the place of smaller air - gap is rotating round with the rotor and therefore the force of unbalanced pull rotating round. As far as the rotor is concerned, the effect will be same, as if the weights were not balanced mechanical, only with the difference that the unbalance is dependent upon the excitation of the machine. The rotating forces also acts on the stator and in high speeds machines produce vibration of the stator frame.

3. Magnetic saturation tends to reduce U.M.P. The pull has a maximum value for a comparatively low state of saturation. For higher saturation, the unbalanced pull falls off. This critical value of induction lies just after the knee of magnetisation curve.

4. There are two factors which enable us to reduce in a machine with fixed principal dimensions the unbalanced pull caused by a definite displacement.

i. The first is to increase the air-gap, because dB/dH for the straight part of the magnetisation curve is very nearly in inverse proportion to the air-gap.

ii. The second means, however, is to reduce the iron section, e.g. that of poles and teeth, because that causes the saturation characteristic to bend earlier, or in other words in auto short the straight part of the magnetisation curve.

3. In bipolar machines, the U.M.P. has different values for displacement in the direction of field axis and right angle to it.

4. The critical speed is lowered by the unbalanced pull and varies with the change in excitation.

C H A P T E R - 4

CALCULATION OF NOISE LEVEL DUE TO HIGH FREQUENCY

FIELD HAVE ASSOCIATE

ROAD

NOISE IN ROTATING MACHINES

4.1. An extremely small amplitude of vibration of a moter frame, of the order of half a micron at usual slot frequencies arround 1000 cycles per seconds, will produce objectionable noise. To avoid this, it is necessary to " balance out" the magnetic forces accurately, to make the laminations, shaft and the frame adequately stiff, and to prevent any natural (resonant) frequencies of the mechanical parts from coinciding with frequencies of the impressed magnetic forces. The actual sound observable some distance away will depend very markedly on the area and the vibration pattern of the surface. To calculate the sound level at any point, therefore, it is necessary first to determine the amplitude and mode of vibration of the surface that give rise to noise, second, to calculate the resultant sound intensity at the surface, and then to calculate the sound intensity at the (distant) point of measurement as determined by the radiation pattern for the particular conditions, and finally, to find the sound level by making allowance for the audibility versus frequency curve of hearing (Fig. 4.1).

4.2. STATOR FRAME VIBRATION

Much of the noise present in rotating machines is due to the poor manufacture. Careless or inaccurate

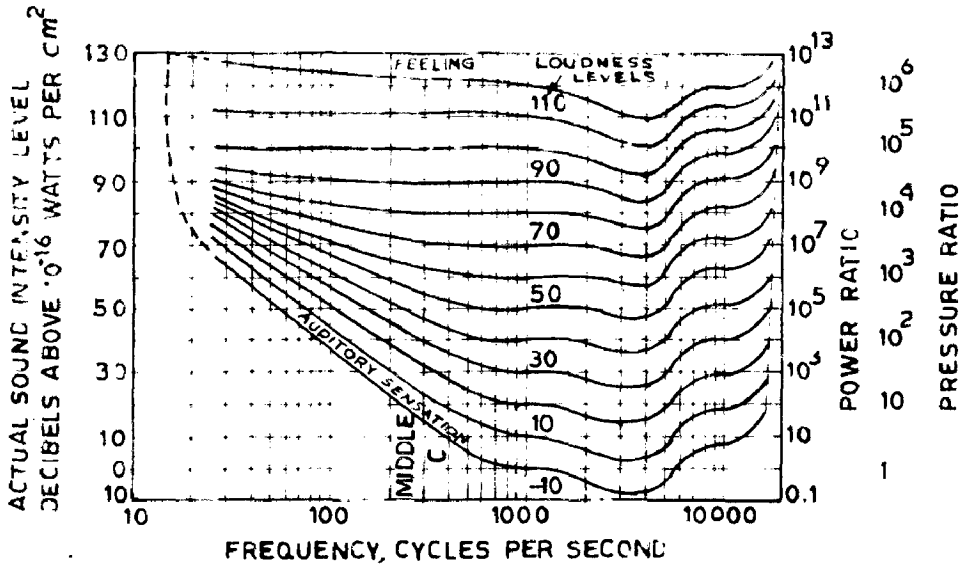

FIG.4.1. LOUDNESS CONTOURS

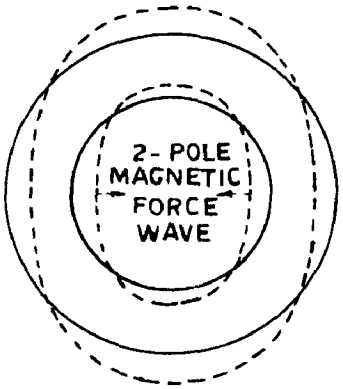

FIG.4.2_FOUR-NODE VIBRATION OF STATOR CORE

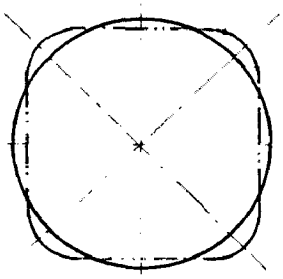

FIG.4.3_DISTORTION OF STATOR DUE TO FOUR POLE TYPE OF PULL

manufacturing methods often show up in some manner as uneven air-gaps, loose bearings, loose rotor bars etc., The radial forces due to the air-gap fields, therefore, are the largest sources of magnetic vibration and noise in Electrical Machines. If the flux were sinusoidally distributed, and there were no flux pulsations, the magnetic force wave around the periphery would be a simple $\sin^2 P\theta$ Curve - that is, a fully displaced sinusoid with twice as many poles of force as there are magnetic poles. The field existing in an air-gap may be roughly classified as follows:

1. Fundamental for which the motor is designed.
2. Stator m.m.f. force harmonics.
3. Stator m.m.f. force sub-harmonics.
4. Rotor m.m.f. force harmonics.
5. Rotor m.m.f. force sub harmonics.
6. Eccentric - gap permeance variation.
7. Stator slot permeance variations.
8. Rotor slot permeance variation
9. Permeance variation due to saturation.

When these fields are superposed on the fundamental flux wave, they give rise to high frequency pulsations in the radial magnetic forces. These may be resolved into a series of sinusoidal force waves with different number of poles, revolving at different speeds, each force wave having twice as many poles as the magnetic field that produces it.

Under these radial forces, the stator frame and the core are set into vibration, in the same manner that a hoop of steel, or a cylindrical bell, responds when struck. If the force - producing magnetic field has two poles, there will be two opposite centres of maximum pull at the poles, and two intermediate points of zero force. The stator will, therefore, be pulled into an elliptical shape, the short axis of the ellipse coinciding with the pole axis, and revolving synchronously with it. This will give a four node vibration (Fig. 4.2). In addition to this, four pole distribution (or any other number) will tend to distort the stator at four (or more) points (Fig. 4.3). That is a 2 P- Pole magnetic field will produce a vibration with 4 P nodes.

It is assumed that the noise- producing force curve for a 2P - pole field is a symmetrical 4P- pole force wave, with a peak value in each direction equal to one half the actual maximum pull at the centre of a magnetic pole. The resultant displacement curve will have a point of inflection at each node, so that there will be zero bending moment at these points. The deflection of the stator can, therefore, be approximated by formulas for the deflection of a beam freely supported at each end, and carrying a sinusoidally distributed load.

For simplicity, the stator 'beam' strength is assumed same as that of a solid steel beam with the same crosssection as the stator yoke, the stiffening due to

stator teeth and frame being neglected. The formula for the deflection of a uniform beam freely supported at both ends and weighted symmetrically with a sinusoidally distributed load is :

$$d = \frac{W L^3}{2\pi^3 E I} = \frac{0.54\ WL^3 \times 10^{-9}}{I} \qquad \ldots(4.1)$$

Where L = Distance between beam supports.

W = Total load in lbs.

E = Modulus of Elasticity = 3×10^7 for Steel.

I = Moment of Inertia of the beam section about its centre line, all in inch units.

To adopt the above formula for noise studies, mean peripheral distance between nodes is substituted for L and I is expressed in terms of stator core depth. Let:

h = radial depth of stator core behind the slots, in inches.

D_s = Mean diameter of the stator core in inches

= D + 2 (slot depth) + 2h

n = One-half the number of modes of core flexure.

= 2P = Number of poles of the force producing magnetic fields.

$$L = \frac{\pi D_s}{2n} = \frac{\pi D_s}{4P} \qquad \ldots(4.2)$$

$$I = \frac{h^3}{12} \text{ per inch of core stacking} \qquad \ldots(4.3)$$

From equations (4.1), (4.2) and (4.3), the radial deflection is :

$$d = \frac{0.25\ W\ D_s^3 \times 10^{-7}}{n^3 h^3} \quad \text{Inches} \quad \ldots(4.4)$$

The above formula is derived from familiar beam theory to give a clear understanding of the problem. The true formulas for deflection of a curved ring under a sinusoidally applied force are :

For 4 nodes , n = 2

$$d = \frac{W\ D_s^3}{6\ E\ h^3} \quad \ldots(4.5)$$

For 6 nodes , n = 3

$$d = \frac{8\ W\ D_s^3}{256\ E\ h^3} \quad \ldots(4.6)$$

For 8 nodes , n = 4

$$d = \frac{W\ D_s^3}{75\ E h^3} \quad \ldots(4.7)$$

It is observed from equations (4.4), (4.5), (4.6) and (4.7) that as n increases, equation (4.4) approaches the correct value; the ratios for 4,6,8 nodes being 0.56, 0.79 and 0.88 . Thus equation 4.4 is true only when n is large.

Since we are interested only in magnetic forces, we can obtain a direct formula by substituting for W its value in terms of peak air-gap flux density. The value of W is half the peak magnetic pull intensity in lbs., per square inch, multiplied by $2/\pi$ and by the pole area.

This gives :

$$W = \frac{1}{3}\left(\frac{1.39\,B^2}{10^8}\right)\left(\frac{2}{\pi}\right)\left(\frac{\pi D}{4P}\right)$$

$$= 0.347\,B^2\,10^{-8}(D/P) \text{ lbs. per inch of core stacking} \qquad \ldots(4.8)$$

Equation No. (4.4) then becomes:

$$d = \frac{1.08\,B^2\,D\,D_s^3 \times 10^{-17}}{P^4 h^3} \text{ inch} \qquad \ldots(4.9)$$

In accordance with equations (4.5), (4.6) and (4.7), the coefficient 1.08 should be replaced by 1.03 for P = 1, by 1.37 for P = 2 and by 1.23 for P = 3 . Equation (4.9) gives the single amplitude of (non resonant) radial vibration of the stator surface due to the force wave of 2P pole magnetic field. With given value of B , h and D, the vibration amplitude varies inversely as the fourth power of the number of poles. Hence in a given machine, only the fields with fewest poles are factors in noise production, in the absence of resonance.

4.3. SOUND RADIATION

The theory of radiation of sound from circular cylinder has been developed by Morse[20]. Morse derives a formula for calculating the sound intensity (S. L) in decibels at a radius 'r' , which is given by the expression:

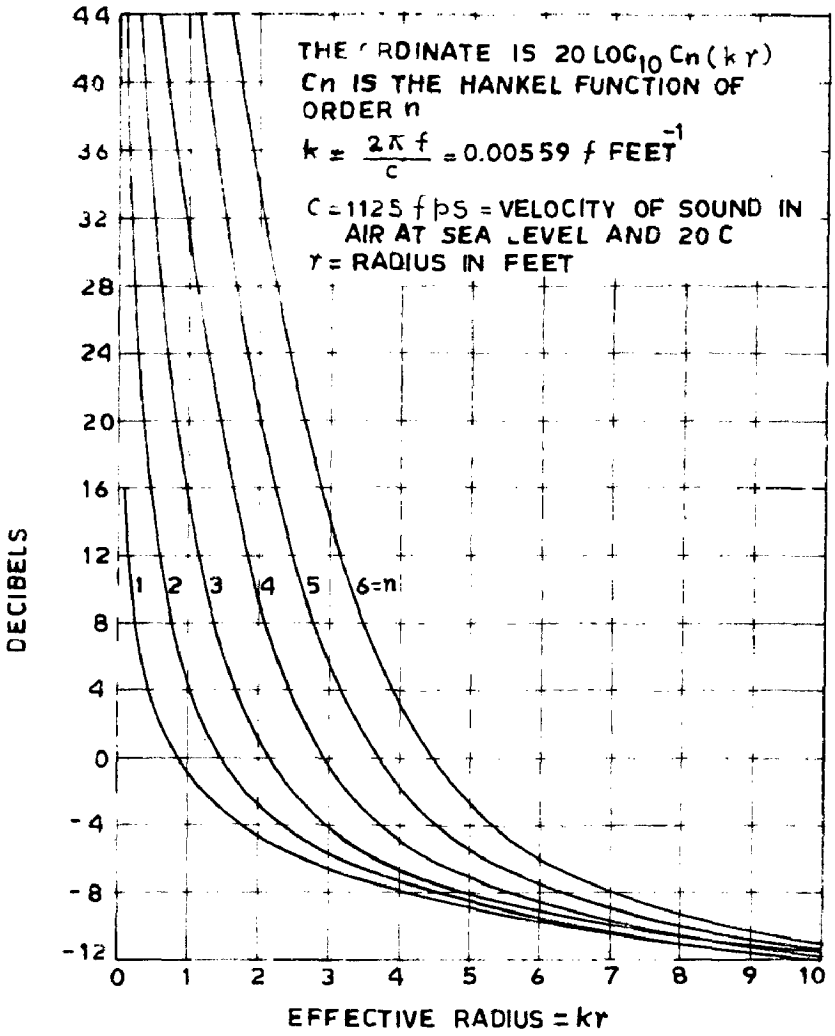

FIG. 4.4 - SOUND RADIATION FROM 2n-NODE VIBRATION OF A CYLINDER

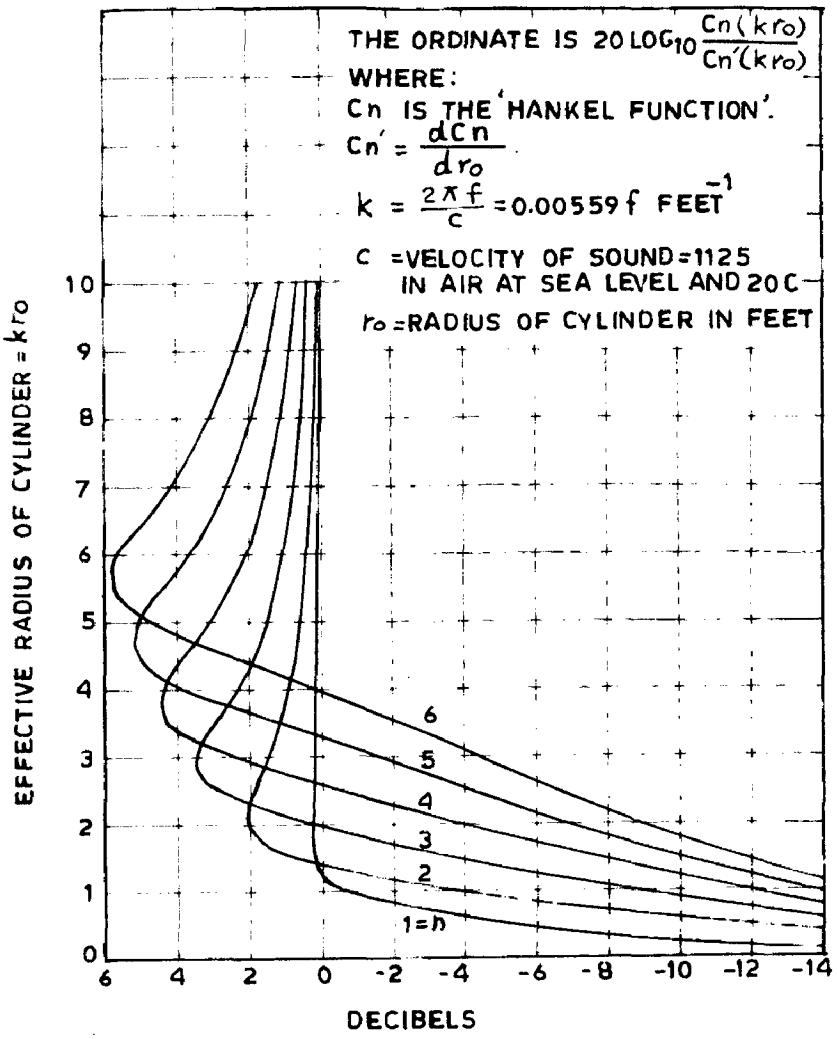

FIG. 4.5_ SOUND INTENSITY DUE TO 2n- NODE VIBRATION OF A CYLINDER

$$S.I. = 131 + 20 \log_{10} \frac{C_n(kr)}{C_n(kr_o)} + 20 \log_{10} \frac{C_n(kr_o)}{C'_n(kr_o)} + 20\log_{10}(\text{sd}$$

... (4.10)

Where

C_n = Absolute value of $J_n + j N_n$, called the Hankel function.

J_n = Bessel function of first kind and nth order

N_n = Neumann function (or a Bessel function of 2nd kind) of the nth order.

C'_n = first derivative of C_n with respect to r_o

r_o = radius of the surface of cylinder in feet

k = $2\pi f / c$ = .00030 f 10^{-1}

c = velocity of sound in air = 1130 fps at 20°C and 760 mm mercury pressure.

The second and third term of the equation No. (4.10) are charted on Figs. 4.4 and 4.5 respectively.

It is evident from the inspection of Fig. 4.4 and 4.5 that, when k r_o is small or when the number of nodes, 2n , is large, the sound intensity decreases with great rapidity as r increases. This again concludes that only magnetic fields with few poles, which produce vibrations with small number of nodes, can be of any importance in noise production.

4.4. CALCULATION OF NOISE DUE TO HIGH FREQUENCY FIELDS

1. If the rotor has R open slots, the air gap permeance will have R complete cycles of variation around the periphery. If the variation is taken to be sinusoidal, the permeance as viewed from the centre of a stator tooth

so

$$P_r = P_o + P_R \text{ Cos } R (\theta - Nt) \qquad \ldots (4.11)$$

Where

P_o = Average permeance.

P_1 = Half amplitude of permeance variation due to the rotor slot.

θ = Angular position of rotor, measured in mechanical radians from the centre of the stator tooth.

N = Rotor speed in mechanical radians per second.

t = Time in second.

R = Number of rotor slot.

ii. The stator slot openings as viewed from the stator, introduce another, stationary , permeance wave.

$$P_s = P_o + P_s \text{ Cos } S \theta \qquad \ldots (4.12)$$

P_o = half amplitude of the stator permeance.

iii. Eccentric air gap introduce another permeance wave, which is given by

$$P_o = P_o + P_1 \text{ Cos } \theta \qquad \ldots (4.13)$$

iv. Permeance variation due to saturation is neglected.

The combine permeance will be product of equations (4.11) (4.12) and (4.13) :

$$P_c = P_r \; P_s \; P_o \qquad \ldots ($$

$$= (P_o + P_1 \text{Cos } \theta)(P_o + P_o \text{ Cos } S \theta)[(P_o + P_R \text{ Cos } R (\theta - Nt)$$

$$= P_o\left[1 + \frac{P_1}{P_o} \text{Cos } \theta\right] \left[1 + \frac{P_o}{P_o} \text{Cos } S\theta\right] \left[1 + \frac{P_R}{P_o} \text{Cos } R (\theta - N$$

$$P_g = P_o \left[1 + A \cos \theta\right]\left[1 + B \cos S\theta\right]\left[1 + c \cos R(\theta - Nt)\right] \quad \ldots (4.14)$$

Where $A = \frac{P_1}{P_o}$, $B = \frac{P_s}{P_o}$, $c = \frac{P_R}{P_o}$ $\quad \ldots (4.15)$

Neglecting all the harmonics, the air gap m.m.f. can be expressed as :

$$a = M' \cos (P\theta - wt) \quad \ldots (4.16)$$

The flux density in the air gap is obtained by multiplying equation No. (4.14) and (4.16) together.

$$B_g = M' P \cos(P\theta - wt) + \frac{M'P_oA}{2}\left\{\cos\left[(P+1)\theta - wt\right] + \cos\left[(P-1)\theta - wt\right]\right\}$$

$$+ \frac{BP_oM'}{2}\left\{\cos\left[(S+P)\theta - wt\right] + \cos\left[(S-P)\theta - wt\right]\right\}$$

$$+ \frac{M'P_oAB}{4}\left\{\cos\left[(S+P+1)\theta - wt\right] + \cos\left[(P-S-1)\theta - wt\right]\right.$$

$$\left. + \cos\left[(P+S-1)\theta - wt\right] + \cos\left[(P-S+1)\theta - wt\right]\right\}$$

$$+ \frac{M'P_oC}{2}\left\{\cos\left[(P+R)\theta - (w+NR)t\right] + \cos\left[(P-R)\theta - (w-NR)t\right]\right\}$$

$$+ \frac{M'P_oBC}{4}\left\{\cos\left[(P+R+S)\theta - (w+NR)t\right] + \cos\left[(P-R-S)\theta - (w-NR)t\right]\right\}$$

$$+ \frac{M'P_oBC}{4}\left\{\cos\left[(P+R-S)\theta - (w+NR)t\right] + \cos\left[(P-R+S)\theta - (w-NR)t\right]\right\}$$

$$+ \frac{M'P_oAC}{4}\left\{\cos\left[(P+R+1)\theta - (w+NR)t\right] + \cos\left[(P-R-1)\theta - (w-NR)t\right]\right\}$$

$$+ \frac{M'P_oAC}{4}\left\{\cos\left[(P+R-1)\theta - (w+NR)t\right] + \cos\left[(P-R+1)\theta - (w-NR)t\right]\right\}$$

$$+ \frac{M'P_oABC}{8}\left\{\cos\left[(P+S+R+1)\theta - (w+NR)t\right] + \cos\left[(P-S-R-1)\theta - (w-NR)t\right]\right\}$$

$$+ \frac{M'P_oABC}{8}\left\{\cos\left[(P+R-S-1)\theta - (w+NR)t\right] + \cos\left[(P-R+S+1)\theta - (w-NR)t\right]\right\}$$

$$+\frac{\Lambda^2 P_0 \Lambda E C}{0}\left\{\cos\left[(P+Q+R-1)\theta-(\omega+NR)t\right]+\cos\left[(P+S+R+1)\theta-(\omega+NR)t\right]\right\}$$

$$+\frac{\Lambda^2 P_0 \Lambda E C}{0}\left\{\cos\left[(P+Q+S+1)\theta-(\omega+NR)t\right]+\cos\left[(P+R+S-1)\theta-(\omega+NR)t\right]\right\}$$

...(4.17)

Squaring the above result and multiplying by a constant will give the radial magnetic pull. Since noise is produced by smaller number of poles (Equation 4.0) , we shall neglect those terms in the force wave having greater number of poles So keeping the fields with smaller number of poles we have :

$$B_G = \Lambda^2 P_0 \cos(P\theta-\omega t)+\frac{\Lambda P_0 \Lambda^2}{8}\left\{\cos\left[(P+1)\theta-\omega t\right]+\cos\left[(P-1)\theta-\omega t\right]\right\}+\frac{\Lambda^2 P_0 \Lambda E C}{0}\left\{\cos\left[(P+Q-S-1)\theta-(\omega+NR)t\right]+\cos\left[(P-Q+S+1)\theta-(\omega-NR)t\right]\right\}$$

...(4.18)

Squaring the above result and dropping the constant terms, which do not contribute to noise, we have :

$$B_G^2 = \left[\frac{\Lambda^2 P_0^2}{8}+\frac{\Lambda^2 P_0^2 \Lambda^2}{4}+\frac{\Lambda^2 B^2 C^2 P_0^2 \Lambda^2}{64}\right]\cos^2(P\theta-\omega t)+\frac{\Lambda^2 P_0^2 \Lambda^2}{8}\left\{\cos 2\left[(P+1)\theta-\omega t\right]+\cos 2\left[(P-1)\theta-\omega t\right]\right\}+\frac{\Lambda^2 B^2 C^2 P_0^2 \Lambda^2}{64\times 8}\left\{\cos 2\left[(P+Q-S-1)\theta-(\omega+NR)t\right]+\cos 2\left[(P-Q+S+1)\theta-(\omega-NR)t\right]+2\cos\left[2(P-1)\theta-2\omega t\right]\right\}$$

$$+\frac{M'^2 P_o^2 A^2}{2}\left\{\cos\left[(2P+1)\theta-2\omega t\right]+\cos\left[(2P-1)\theta-2\omega t\right]\right\}$$

$$+\frac{A^2 P_o^3 M'^3 EC}{30}\left\{\cos\left[(2P+R-S)\theta-(2\omega+RN)t\right]+2\cos\left[(R-S-2)\theta-RNt\right]\right.$$

$$+\cos\left[(2P-R+S+2)\theta-(2\omega-RN)t\right]+2\cos\left[(R-S)\theta-RNt\right]$$

$$\left.+\cos\left[(2P+R-S-2)\theta-(2\omega+RN)t\right]+\cos\left[(2P-R+S)\theta-(2\omega-RN)t\right]\right\}$$

$$+\frac{M'^2 P_o^2 ABC}{30}\left\{\cos\left[(2P+R-S+1)\theta-(2\omega+RN)t\right]+\cos\left[(2P-R+S+1)\theta\right.\right.$$

$$\left.\left.-(2\omega-RN)t\right]+2\cos\left[(R-S-1)\theta-RNt\right]\right\}$$

...(4.10)

4.3. ILLUSTRATIVE EXAMPLE

To calculate the noise level due to these high frequency fields, let us take an example of 5 H.P. Induction motor with S = 36 , R = 44 and P = 2

Stator slot opening = 3 mm

Rotor slot opening = 1 mm

Length of air gap = 0.45 mm

$A = \frac{P_A}{P_o} = 0.302$ (From equation 3.10 and 3.11).

D = .35 , δ = 0.3 , D = 3.5" , h = 0.833"

D_o = 5.55" Outer diameter = D_o = 9.23"

i. Taking the second field, for example, with 4 poles, at a frequency = 100 cycles, the magnitude as compared to the fundamental 4 P - pole force wave is given by the

ratio of their coefficients in equation (4.10).

$$\frac{B_0^2 \text{ of } 4 \ (P=1) \text{ Pole wave}}{B_0^2 \text{ of } 4 \ P \text{ Pole wave}} = \frac{\frac{A^2 D_{0.1}^2 \cdot 3}{8}}{\frac{H^2 b_0^2}{3} + \frac{A^2 B_0^2 H^2 \cdot 3}{4} + \frac{A^2 B^2 C^2 D_{0.1}^2 \cdot 3}{64}}$$

$$= 0.03$$

In Equation (4.8), putting the harmonic number of (Zero) Pole pai poles 2 ($P=1$) = 2, in place of 2 P, we have

$$J = .03 \times .307 \, B_0^2 \times 10^{-8} \, \frac{2D}{2(P-1)} \text{ lbs / in of core length}$$

$$J = .03 \times .307 \, (3000)^2 \times 10^{-8} \times 3.0 = 0.333 \text{ lb/inch of core lengt}$$

and from equation (4.4), we have

$$d = \frac{0.20 \, J \, B_0^2}{n^2 D^2} \times 10^{-7} = 2.1 \times 10^{-8} \text{ inch.}$$

$$\text{At } r_0 = .0030 \times 100 \times \frac{0.20}{2n12} = 0.320$$

and at any radius $r = 10^n$

$$\text{At } r = .0030 \times 10 \, (\tfrac{10}{12}) = 0.780$$

From Equation No. (4.10), Figs (4.4) and (4.5), the sound intensity at an 10" radius is :

$$S.I. = 130 + (0 - 20) - 10 + 20 \log_{10} (3 \times 2.1 \times 10^{-8} \times 100)$$

$$= 0.0 \text{ dB.}$$

This is far below the limit of hearing at 100 cycles. We conclude, therefore, that the 100 cycle noise of a small polyphase motor is inaudible, unless mechanical resonance

occurs.

11. Let us now consider the field with number of poles Δ_0 at a frequency = 1000cycles.

B_0^2 of (2D-2S-4D-4) Pole wave $= \frac{A^2 P_0^2 H'^2 E^2 C}{32}$

J_0^2 of 4 P - Pole wave $= \frac{H'^2 P_0^2}{8} + \frac{A^2 P_0^2 H'^2}{4} + \frac{A^2 B^2 C^2 P_0^2 H'^2}{64}$

$= 0.0016$

$W = 0.0016 \times 0.367 \times (30000)^2 \times 10^{-20} \frac{2D}{(D-S-2P-2)}$

$= .0233$ lbs/ inch of core length.

$d = .33 \times .0233 \left(\frac{0.00}{2\pi.033}\right)^2 \times 10^{-7} = 00.3 \times 10^{-7}$

$\log P_0 = 3.30$

$\log r = 7.00$

Therefore S. L. = 101 - 11 + 3.3 + 2 - 74.0 = 40.7 dB.

From Fig. 4.10 the corresponding sound level is 40 dB It is therefore evident that this 1000 cycle noise can be a cause of serious annoyance with four pole field.

The other expected force waves from equation (4.10) are :

a. A 4P = 0 mode wave at a frequency = 2 f = 100 cycles

b. A 4(P+1) = 12 mode wave of a freq. = 3 f = 100 cycles

c. A4(P-1) = 4 mode wave at a freq. = 3 f = 100 cycles.

d. A 4 (P + R - S - 1) = 30 mode wave at a frequency

$= \left(1 + \frac{P}{S}\right) 3f = 3300$ cycles.

o A 4 (B - S - P - 1) = 20 mdo vavo ot o frequency

= ($\frac{3}{5}$ -1) 3 f = 3100 cycles.

f. A 4 (B - S - 1) = 20 mdo vavo ot o frequency

= 3 $\frac{3}{5}$ f = 3000 cycles.

C. A 3 (3P + 1) = 10 mdo vavo ot a freq. 3 f = 100 cycles.

D. A 3 (3P - 1) = 0 mdo vavo ot a freq. = 3f = 100 cycles.

E. A 3(3P+D-3) = 30 mdo vavo ot a freq. (3+$\frac{3}{5}$)f = 3000 cycles.

J. A 3 (D-S-3) =12 mdo vavo ot a freq. =$\frac{3}{5}$ f = 1100 cycles.

H. A 3(D-S-3P-3) =6 mdo vavo ot a freq. =($\frac{3}{5}$ -3)f =1000 cycles.

I. A 3(D-S) =10 mdo vavo ot a freq. = $\frac{3}{5}$ f = 1100 cycles.

K. A 3(3P+D-S-3) =30 mdo vavo ot a freq. =(3+$\frac{3}{5}$)f =3000cycles.

L. A 3 (3P - B + 3) = 0 mdo vavo ot a fre q.

= ($\frac{3}{5}$ -3) f = 1000 cycles.

M. A. 3 (3P+D-S-1) = 30 mdo vavo ot a frequency

= ($\frac{3}{5}$ +3) f = 3100 cycles.

N. A 3(D-S-3P-1) = 6 mdo vavo ot a frequency

= ($\frac{3}{5}$ -1) f = 1000 cycles

O. A 3 (D-S-1) = 10 mdo vavo ot a frequence

= -$\frac{3}{5}$ f = 1100 cycles.

.... (4.20)

The field with n = 0 and n = 0 will produce for zero case. in comparision with n = 2 .

4.0. FORCE LAWS FOR CONCENTRIC ROTOR

Neglecting the effect of rotor eccentricity , the force wave can be expressed as :-

$$F_0^2 = \left[\frac{p^2 u_1^2}{2} + \frac{p^2 u_1^2 E^2}{4} + \frac{p^2 c^2 u_1^2}{4} + \frac{u_1^2 p^2 E^2 c^2}{16}\right] \cos 2(\omega - \omega t)$$

$$+ \frac{p_o^2 c^2 u_1^2}{2}\left\{\cos 2\left[(\omega - p)\theta + (v - \omega_r)t\right]\right\}$$

$$+ p_o^2 u_1^2 Ec\left\{\cos\left[(\omega - p)\theta - \omega_r t\right]\right\}$$

$$+ \frac{p_o^2 u_1^2 Ec}{2}\left\{\cos\left[(2p + \omega - s)\theta - (2v + \omega_r)t\right]\right\}$$

$$+ \frac{p_o^2 u_1^2 Ec}{2}\left\{\cos\left[(\omega - 2p)\theta + (2v - \omega_r)t\right]\right\}$$

.... (4.21)

For the same rotor and stator slot combinations, the expected force wave without eccentricity are

a. A 4P = 8 mode wave at a freq. = 2 f = 100 cycles.

b. A 4(P-S-P) = 24 mode wave at a freq $= \left(\frac{3}{2} - 1\right) f$ = 1000 c/s

c. A 2(P-S) =12 mode wave at a freq = $\frac{3}{2} f$ = 1500 c/s

d. A 2(2P+P-S) = 24 mode wave at a freq. $= \left(\frac{3}{2} + 1\right) f$ =1500 c/s

e. A 2 (P-S- 2P) = 0 mode wave at a frequency

$$= \left(\frac{2}{p} - 1\right) f \quad = 1000 \text{ cycles.}$$

... ... (4.22)

6.7 CONCLUSION

From equation (6.30) and (6.32), it is evident that the effect of rotor eccentricity is to produce 6.0, 10 radial force wave in addition to 0.10 and 20 radial which are already existing in the machine with concentric air-gap, for the same stator-rotor slot combinations. Since the sound intensity is proportional to 'd' and 'd' varies inversely as the fourth power of number of radial. Hence in the absence of resonance, the field with smaller radial will produce more noise. The machine with eccentric rotor therefore, will produce more noise than with concentric rotor.

If during acceleration, the motor reaches such a speed at which the rotor frequency coincides with the stator resonance the amplitude of stator resonance will increase so much that rotor may strike the stator and magnetic noise may be very loud.

B I B L I O G R A P H Y

1. Fisher-Hinnen, J.:"Dynamo Design" pp. 260-265 (Van-Nostrand) 1899.

2. Behrend, B.A.: " On the Mechanical Forces in Dynamos caused by Magnetic Attraction". Trans.AIEE, Vol 18,pp.671-626, Nov. 1900.

3. Knowlton, Edgar , " Magnetic attraction in Dynamos due to Armature and Field being non-concentric". Electrical World and Engineer Vol. 37, pp.969-970,June 1901.

4. J.Rey, "Magnetic Pull Due to Eccentricity of Rotor of Induction Motors", L' Eclairage Electrique, Vol.38, pp.281-285, Feb 1904; Vol.41, pp.257-260,Nov,1904.

5. Sumec, J.K., " Determination of Magnetic pull on Rotor due to Eccentricity" Zeitschriff fur Elektrotechnik,Vol. 22, pp. 727-728. Dec. 1904.

6. Soschinski, B; " Pull due to Rotor Eccentricity" Zeitschriff fur Elecktrotechnik, pp. 183, Mar, 1905.

7. F. Niethammer, " Lateral Magnetic pull of Dynamos and Motors" Zeitschriff fur Electrotechnik, Vol .23,pp.421-22, July 1905; L' Eclairage Electrique, Vol.44, pp. 154-755, July 1905.

8. Moore, C.R.: " A Study of Unbalanced Pull" Electrical Review and Western, Electrician, Vol.58,pp.83-86,Jan,1911.

9. Walker Miles:" Specification and Design of Dynamo-Electric Machinery" pp. 57-62, 347, 416,452,:(Longmans, Green,) 1915.

10. Rosenberg, E. : " Magnetic Pull in Electrical Machines", A. I. E. E. Trans, Vol. 37, 1918, pp 1425-69.

11. Robinson, R.C. : " The Calculation of Unbalanced Magnetic Pull in Synchronous Induction Motors". A. I. E. E. Trans, Vol, 62, 1943, pp. 620-24.

12. Covo, A. : "Unbalanced Magnetic Pull in Induction Motors With Eccentric Rotors" A. I. E. E. Trans, Vol. 73, Part III-B, 1954, pp 1421-25.

13. Friese, W and Jordan, H., " One Sided Magnetic Pulling Force in Three phase Machines". Electrotech, Z (E. T. Z.) A (Germany), Vol. 83, No. 9, pp. 299-303. April 23, 1962.

14. Swann, S. A. " Effect of Eccentricity on the Magnetic Field in the Air-gap of a Non salient Pole Machine" Proc. I. E. E., Vol 110, No. 5, May 1963, pp. 903-15.

15. Durell, C. V. : " Modern Geometry" (Macmillan, 1938) Chapter 9.

16. Pipes, L. A., : " Applied Mathematics for Engineers and Physicists" (McGraw Hill, 1946), Chap. 20, Article 7.

17. Whittaker, E. T., and Robinson, G. : " The calculus of Observations" (Blackie, 1940), p. 273.

18. Godfrey, C. and Siddons, A. W. : " Modern Geometry" p. 87-93.

19. Graham, C, Beckwith, S, and Milliken, F. H. : " Magnetic Noise in Synchronous Machines", A. I. E. E. Trans., Vol. 50, Sept 1931, pp 1056-62.

20. Morse, P.M. : " Vibration and Sound", Second Edition McGraw Hill, 1948.

21. Alger, P.L., " The Nature of Polyphase Induction Machines" (Chapman & Hall Limited: London).

22. Hildebrand, L.E., " Quiet Induction Motors" A. I.E.E. Trans, Vol 49, July 1930, pp 848-52.

23. Langsdorf, S. Alexander " Theory of Alternating Machinery" (McGraw Hill Book Company).

APPENDIX I

FOURIER ANALYSIS OF M.M.F. DISTRIBUTION

Two special cases that are frequently encountered are concerned with the space distribution of m.m.f. of a single coil of the armature winding. In one of these cases, the coil is of full pitch, i.e., its throw or spread is from centre to centre of the adjacent poles; in the other case, the coil has fractional pitch, its throw being less than the pole pitch. In both cases it is customary to assume that when the coil is carrying current the point by point distribution of the m.m.f. (in space time) is represented by a straight line as in Figs. 1-A and 1-B. The justification of this assumption is that the m.m.f. of a coil is by definition equal to the work required to carry a unit magnet pole once around any closed path linking with the coil, and since that part of such a path has negligible reluctance in comparison with that of air-gap, the effective m.m.f. acting on the air-gap remains substantially constant throughout the coil spread. Let the constant m.m.f. be M.

In all the cases that arise in practice, the curves showing the point by point variation of these quantities are periodic and single valued and may therefore be resolved into a fundamental and higher harmonics. In the general case, which we are concerned, the dependent variable y can be expressed as a function of the independent variable θ between the limits 0 and π by the equation -

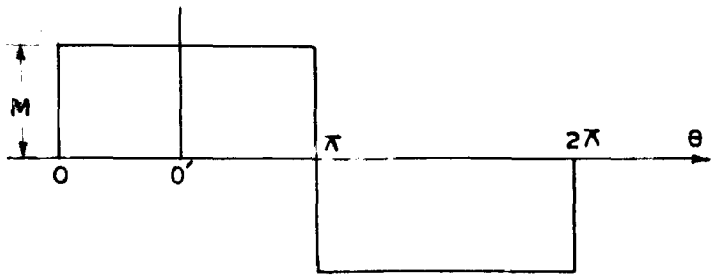

FIG.1-A_FULL PITCH RECTANGULAR DISTRIBUTION OF M.M.F.

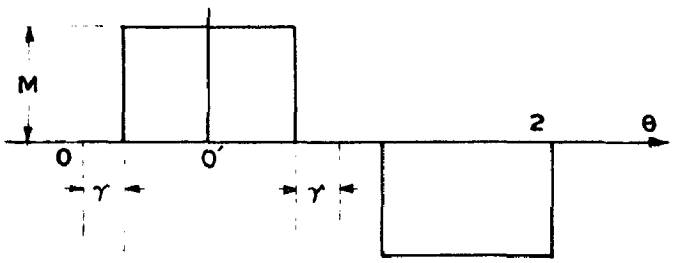

FIG.1-B_FRACTIONAL PITCH RECTANGULAR DISTRIBUTION OF M.M.F.

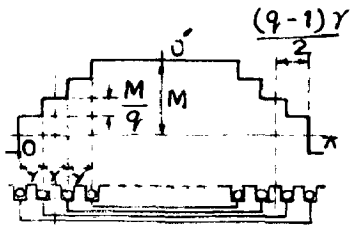

FIG.1-C_STEPPED DISTRIBUTION OF m m f

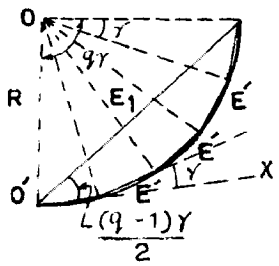

FIG.1-D_COMPONENT EMFS OF DISTRIBUTED WINDING

$$y = f(\theta) = A_1 \sin\theta + A_2 \sin 2\theta + A_3 \sin 3\theta + \ldots + A_n \sin n\theta + B_1 \cos\theta + B_2 \cos 2\theta + B_3 \cos 3\theta + \ldots + B_n \cos n\theta \quad \ldots (1)$$

Where the coefficients are given by

$$A_n = \frac{2}{\pi} \int_0^{\pi} f(\theta) \sin n\theta \, d\theta \quad \ldots (2)$$

$$B_n = \frac{2}{\pi} \int_0^{\pi} f(\theta) \cos n\theta \, d\theta \quad \ldots (3)$$

a. CONCENTRATED COILS, FULL AND FRACTIONAL PITCH:

Two types of windings of basic importance have been shown in Figs 1-A and 1-B . They are the concentrated windings of full pitch and fractional pitch.

In Fig. 1-A , we have

$y = M$ between $\theta = 0$ and $\theta = \pi$

$y = -M$ between $\theta = \pi$ and $\theta = 2\pi$

$$A_n = \frac{2}{\pi} \int_0^{\pi} M \sin n\theta \, d\theta = \frac{4M}{\pi n} \text{ when n is odd} \quad \ldots (4)$$

$= 0$ when n is even

Since the average height of the wave is zero. $B_o = 0$ Also $B_n = 0$, because y changes sign when θ passes through zero.

∴ The m.m.f. distribution of a full pitch concentrated winding can be expressed as : -

$$a = \frac{4M}{\pi} \left[\text{Sin}\Theta + \frac{1}{3}\text{Sin}\,3\Theta + \frac{1}{5}\text{Sin}5\Theta + \ldots \frac{1}{(2n+1)}\text{Sin}(2n+1)\Theta \right]$$

If the m.m.f. distribution has rectangular wave form with P number of pole pairs -

$$a = \frac{4M}{\pi} \sum_{n=0}^{\infty} \frac{\text{Sin}\,(2n+1)P\Theta}{(2n+1)P} \qquad \ldots(5)$$

The m.m.f. distribution referring to the origin O' is given by

$$a = \frac{4M}{\pi} \sum_{n=0}^{\infty} \frac{(-1)^n \text{Cos}\,(2n+1)P\Theta}{(2n+1)P} \qquad \ldots(6)$$

The fractional pitch coil of Fig. 1-B represents a function y in which

$y = 0$ between $\Theta = o$ and $\Theta = \gamma$

$y = M$ between $\Theta = \gamma$ and $\Theta = \pi-\gamma$

$y = 0$ between $\Theta = \pi-\gamma$ and $\Theta = \pi$

From equation No. 2 , we have

$$A_n = \frac{2}{\pi}\left[\int_0^{\gamma} 0\text{Sin}\,nP\Theta\,d\Theta + \int_{\gamma}^{\pi-\gamma} M\text{Sin}nP\Theta\,d\Theta + \int_{\pi-\gamma}^{\pi} 0\text{Sin}Pn\Theta\,d\Theta\right]$$

$$A_n = \frac{4}{\pi}\,\frac{M}{nP}\,\text{Cos}\,n\gamma \qquad \text{when n is odd (n=0, 1, 3..)}$$

$$\text{or } A_n = \frac{4M}{\pi} \sum_{n=0}^{\infty} \frac{\text{Cos}(2n+1)P\gamma}{(2n+1)P} \qquad \ldots(7)$$

$B_n = 0$ from equation (3)

∴ M.M.F distribution having P number of pole-pairs of a fractional pitch winding can be expressed as :

$$a = \frac{4\Pi}{\pi P} \sum_{n=0}^{\infty} \frac{\cos (2n+1) PY}{(2n+1)} \sin (2n+1) PO \quad \ldots (8)$$

$$= \frac{4\Pi}{\pi P} \cos PY \sin PO + \frac{1}{3} \cos 3PY \sin 3PO + \frac{1}{5} \cos 5PY \sin 5PO$$
$$+ \ldots + \frac{\cos (2n+1) PY}{(2n+1)} \sin (2n+1) PO$$

$$\ldots (9)$$

Referring to origin 0° , we have

$$a = \frac{4\Pi}{\pi} \sum_{n=0}^{\infty} \frac{(-1)^n \cos (2n+1) PY \cos (2n+1) PO}{(2n+1) P} \quad \ldots (10)$$

b. STEPPED DISTRIBUTION:

Case 1. If the winding is distributed in slots in the manner indicated in the lower part of Fig 4-C , each of the individual coils will contribute a rectangularly distributed m.m.f. of the type discussed in "a" . If the outer pitch coil is assumed to have the same number of turns as the inner fractional-pitch coils, the resultant m.m.f. of all the component rectangular distributions will be the same, namely, Π / q , where q is the number of the coils in the group.

Referring to equations (8) and (9), the amplitude of the nth harmonic of the successive coils, beginning with the outer full pitch coil , are, respectively:

Coil	Amplitude
1 (outer)	$\frac{4}{\pi} \frac{\Pi}{q} \frac{1}{(2n+1)P}$
2	$\frac{4}{\pi} \frac{\Pi}{q} \frac{\cos (2n+1) PY}{(2n+1) P}$
3	$\frac{4}{\pi} \frac{\Pi}{q} \frac{\cos 3 (2n+1) PY}{(2n+1) P}$

$$q(2n+1)\pi \qquad \frac{4}{\pi}\frac{N}{q}\,\frac{\cos\left[(q-1)(2n+1)\frac{\gamma}{2}\right]}{(2n+1)\frac{\gamma}{2}}$$

Hence, the resultant amplitude of the nth harmonic is the sum of the terms listed above. This sum is given by

$$A_n = \frac{4}{\pi}\frac{N}{q}\,\frac{1}{(2n+1)\frac{\gamma}{2}}\left[1+\cos(2n+1)\gamma+\cos 2(2n+1)\gamma+\ldots+\cos(q-1)(2n+1)\gamma\right] \qquad \ldots(11).$$

If the N turns of the original concentrated winding be distributed in q slots / pole, and let γ be the angle (in electrical degrees) between the adjacent slots of a group. If E be the e.m.f. that would be generated by the entire group of N turns if they were concentrated in a single slot, the e.m.f. due to N / q turns/slot will be $E/q = E'$. If the e.m.f. due to the coils in the first slot of the successive groups is represented in a complex notation by E', that of the second will be out of phase with it by an angle γ and therefore can be represented by $E' e^{j\gamma}$

∴ The resultant e.m.f. is given by

$$E_1 = E'\left(1+e^{j\gamma}+e^{j2\gamma}+\ldots\ldots+e^{j(q-1)\gamma}\right)$$

$$E_1 = E'\,\frac{e^{jq\gamma}-1}{e^{j\gamma}-1}$$

$$E_1 = E' \frac{(\text{Cos } q\gamma - 1) + j \text{ Sin } q\gamma}{(\text{Cos } \gamma - 1) + j \text{ Sin } \gamma}$$

The real value of E_1 is therefore -

$$E_1 = E' \sqrt{\frac{(\text{Cos } q\gamma - 1)^2 + \text{Sin}^2 q\gamma}{(\text{Cos } \gamma - 1)^2 + \text{Sin}^2 \gamma}}$$

$$E_1 = \frac{E}{q} \frac{\text{Sin } (q\gamma/2)}{\text{Sin } \gamma/2} \qquad \ldots (12).$$

The geometrical significance of equation (12) is shown in Fig. 1-D.

Let us consider the cosine and sine series given below : -

$$1 + \text{Cos } \gamma + \text{Cos } 2\gamma + \ldots\ldots + \text{Cos } (q-1)\gamma$$

$$\text{Sin}(0) + \text{Sin } \gamma + \text{Sin } 2\gamma + \ldots\ldots + \text{Sin } (q-1)\gamma$$

If the cosine series is multiplied by $E' = E/q$, the terms are represented to the scale by the projection upon O'X of the successive chords of Fig. 1-D. Their sum is, therefore, the projection upon O'X of the geometrical sum of the chords themselves, i.e., of E_1.

$$\text{i.e. } E'\left[1 + \text{Cos } \gamma + \text{Cos } 2\gamma + \ldots\ldots + \text{Cos } (q-1)\gamma\right] = E_1 \text{Cos}(q-1)\gamma/2$$

$$\ldots (13).$$

From Equation Nos. (12) and (13), we have

$$1 + \text{Cos } \gamma + \text{Cos } 2\gamma + \ldots + \text{Cos}(q-1)\gamma = \frac{\text{Sin}(q\gamma/2)}{\text{Sin}(\gamma/2)} \text{Cos}(q-1)\gamma/2$$

$$\ldots (14)$$

Similarly, the sum of the same series (if multiplied by E') represents the projection of E_1 upon an axis perpendicular to O'K, whence

$$\sin\gamma + \sin 2\gamma + \ldots + \sin(q-1)\gamma = \frac{\sin(q\gamma/2)\,\sin((q-1)\gamma/2)}{\sin(\gamma/2)} \qquad \ldots(16)$$

From Equation No. (12) and (13), we have

$$A_n = \frac{4}{\pi}\,\frac{H}{(2n+1)P}\,\frac{1}{q}\,\frac{\sin\left[\frac{q(2n+1)P\gamma}{2}\right]\cos\left[(q-1)(2n+1)P\gamma/2\right]}{\sin\left[\frac{(2n+1)P\gamma}{2}\right]} \qquad \ldots(16)$$

$$\therefore\quad e = \sum_{n=0}^{\infty}\frac{4H}{\pi(2n+1)P}\,\frac{\sin\left[\frac{q(2n+1)P\gamma}{2}\right]\cos\left[(q-1)(2n+1)P\gamma/2\right]}{q\sin\left[\frac{(2n+1)P\gamma}{2}\right]}\,\sin(2n+1)P\theta$$

$$\ldots(17).$$

Referring to origin O', we have.

$$e = \frac{4H}{\pi}\sum_{n=0}^{\infty}\frac{(-1)^n\sin\left[\frac{q(2n+1)P\gamma}{2}\right]\cos\left[(q-1)(2n+1)P\gamma/2\right]}{q\sin\left[\frac{(2n+1)P\gamma}{2}\right]}\cdot\frac{\cos(2n+1)P\theta}{(2n+1)P} \qquad \ldots(18)$$

Case 3: Fig. 1-E illustrates a distributed winding, arranged in slots, with the outer coil of less than full pitch, but with all coils having the same number of turns. This case occurs in the rotor windings of Turbo-alternators and in the stator windings of generators and motors. It follows from equation no. that the amplitudes of the nth harmonic of the several coils are given by the following table:

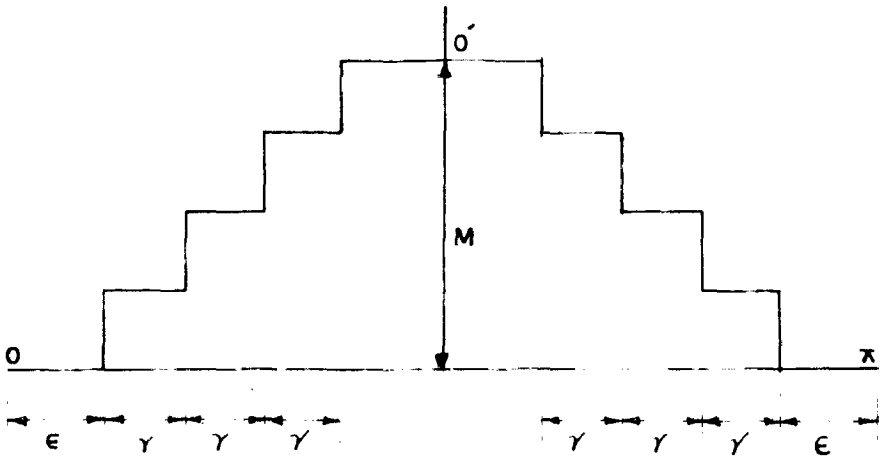

FIG.1-E_STEPPED DISTRIBUTION, FRACTIONAL PITCH

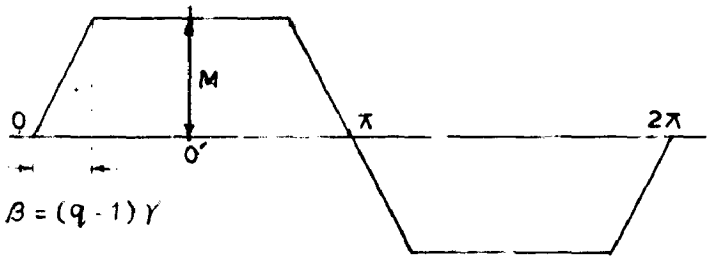

FIG. 1-F_TRAPEZOIDAL DISTRIBUTION, FULL PITCH

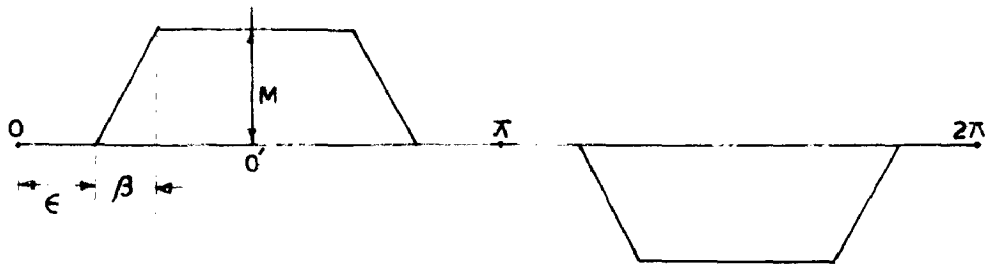

FIG.1-G_TRAPEZOIDAL DISTRIBUTION, FRACTIONAL PITCH

Coil	Amplitude.
1(Outer)	$\frac{4}{\pi}\frac{M}{q}\frac{\cos(2n+1)\beta e}{(2n+1)\beta}$
2	$\frac{4}{\pi}\frac{M}{q}\frac{\cos(2n+1)\beta(e+\gamma)}{(2n+1)\beta}$
3	$\frac{4}{\pi}\frac{M}{q}\frac{\cos(2n+1)\beta(e+2\gamma)}{(2n+1)\beta}$
----	---------
q	$\frac{4}{\pi}\frac{M}{q}\frac{\cos(2n+1)\beta(e+(q-1)\gamma)}{(2n+1)\beta}$

The amplitude of the nth harmonic of the composite curve of fig 1-E is then the sum of the above terms or

$$A_n = \frac{4}{\pi}\frac{M}{(2n+1)\beta}\frac{1}{q}\cos(2n+1)\beta e\left[1+\cos(2n+1)\beta\gamma + \cos 2(2n+1)\beta\gamma + \ldots + \cos(q-1)(2n+1)\beta\gamma\right] - \sin(2n+1)\beta e\left[\sin(2n+1)\beta\gamma + \sin 2(2n+1)\beta\gamma + \ldots + \sin(q-1)(2n+1)\beta\gamma\right] \quad \ldots(10)$$

From Equation No. (14), (15) and (10), we have

$$A_n = \frac{4}{\pi}\frac{M}{q(2n+1)\beta}\frac{\sin\left[q(2n+1)\beta\gamma/2\right]}{\sin\left[(2n+1)\beta\gamma/2\right]}\left[\cos(2n+1)\beta e\cos\frac{(q-1)(2n+1)\beta\gamma}{2} - \sin(2n+1)\beta e\sin\frac{(q-1)(2n+1)\beta\gamma}{2}\right]$$

$$A_n = \frac{4}{\pi} \frac{\Delta_1}{(2n+1)P} \frac{\sin\left[q\,(2n+1)\,P\,\gamma/2\right]}{q \sin\left[\frac{(2n+1)P\gamma}{2}\right]}$$

$$\cos\,(2n+1)\,P\left[\theta + \frac{(q-1)\,\gamma}{2}\right] \qquad \ldots(20)$$

$$\theta = \frac{4\Delta_1}{\pi P}\left\{\frac{\sin\frac{qP\gamma}{2}}{q \sin\frac{P\gamma}{2}} \cos P\left[\theta + \frac{q-1}{2}\gamma\right] \sin P\theta\right.$$

$$+ \frac{\sin q\frac{3P\gamma}{2}}{q \sin\frac{3P\gamma}{2}} \cos 3P\left[\theta + \frac{q-1}{2}\gamma\right] \frac{\sin 3P\theta}{3}$$

$$+ \ldots\ldots + \frac{\sin\left[q\,(2n+1)\frac{P\gamma}{2}\right]}{q \sin\frac{(2n+1)P\gamma}{2}} \cos\,(2n+1)P\left[\theta + \frac{q-1}{2}\gamma\right]$$

$$\left.\frac{\sin\,(2n+1)P\theta}{(2n+1)}\right\} \qquad \ldots(21).$$

Referring to origin O' , we have

$$\theta = \frac{4\Delta_1}{\pi} \sum_{n=0}^{\infty} (-1)^n \frac{\sin q(2n+1)\frac{P\gamma}{2}}{q \sin\frac{(2n+1)P\gamma}{2}} \cos\,(2n+1)P\left[\theta + \frac{q-1}{2}\gamma\right]$$

$$\frac{\cos\,(2n+1)P\theta}{(2n+1)P} \qquad \ldots(22)$$

---

6. TRANSVERSAL DISTRIBUTION

Case 1 : *Full Pattern* : If the width of Fig 6-C is considered more and more by successively increasing the

number of coils and slots in the belt having angular width $\beta = (q-1)\gamma$, the stepped diagram will approach as a limit the trapezoidal form of Fig 1-7 . The amplitude of any harmonic of this distribution may then be found from Equation (10) by determining the limiting value of the factor when q approaches infinity and γ approaches zero, subjected to the condition that $(q-1)\gamma = \beta = \text{Constant}$. The result is

$$A_n = \frac{4}{\pi} \frac{H}{(2n+1)p} \frac{\sin (2n+1)p\beta/2 \cos (2n+1)p\beta/2}{(2n+1)p\beta/2}$$

$$A_n = \frac{4}{\pi} \frac{H}{\beta (2n+1)^2 p^2} \sin (2n+1)p\beta \qquad \ldots (23)$$

Hence the complete equation for the full pitch trapezoidal distribution is, therefore , -

$$a = \frac{4}{\pi} \frac{H}{\beta p^2} \left[\sin p\beta \sin p\theta + \frac{\sin 3p\beta \sin 3p\theta}{9} + \frac{\sin 5\beta}{25} \sin 5\theta + \ldots + \frac{\sin (2n+1)p\beta}{(2n+1)^2} \sin (2n+1)p\theta \right] \qquad \ldots (24)$$

Referring to origin O' , we have

$$a = \frac{4H}{\pi} \sum_{n=0}^{\infty} (-1)^n \frac{\sin (2n+1)p\beta}{(2n+1)\beta} \frac{\cos (2n+1)p\theta}{(2n+1)p} \qquad \ldots (25)$$

Case 2 - Fractional Pitch : - The curve shown in Fig. 1-7 is that of a uniformly distributed winding of less than full pitch spread. It is clearly a special case of stepped distribution of Fig 1-6 . Since it may be derived from the

latter by indefinately increasing the number of steps q, subjected to the condition $(q-1)\gamma = \beta$. The limiting form of equation (20) is

$$A_n = \frac{\Delta}{\pi} \frac{M}{(2n+1)P} \frac{\sin \frac{(2n+1)P\beta}{2} \cos (2n+1)P(\theta + \beta/2)}{(2n+1)P\beta/2}$$

$$A_n = \frac{\delta}{\pi} \frac{M}{\beta (2n+1)^2 P^2} \sin (2n+1)\beta/2 \cos (2n+1)P(\theta+\beta/2) \quad \ldots(26)$$

Which is the amplitude of the nth harmonic of the fractional pitch trapezoidal distribution

∴ Complete equation for the fractional pitch trapizoidal distribution is given by

$$a = \frac{\delta}{\pi} \frac{M}{\beta} \frac{1}{p^2} \left[\sin \beta/2 \cos P(\theta+\beta/2) \sin P\theta + \frac{\sin 3\beta/2 \cos 3P(\theta+\beta/2) \sin 3P\theta}{9} + \frac{\sin 5\beta/2 \cos 5P(\theta+\beta/2) \sin 5P\theta}{25} + \ldots + \frac{\sin (2n+1)\beta/2 \cos (2n+1)P(\theta+\beta/2) \sin (2n+1)P\theta}{(2n+1)^2} \right]$$

Referring to origin O' we have ....(27)

$$a = \frac{2M}{\pi} \sum_{n=0}^{\infty} (-1)^n \frac{\sin (2n+1)\beta/2 \cos (2n+1)P(\theta+\frac{\beta}{2})}{(2n+1)P\beta} \cdot \frac{\cos (2n+1)P\theta}{(2n+1)P} \quad \ldots(28)$$

--

APPENDIX 2

SOME DEFINATIONS

1. ORTHOGONAL CIRCLES

Two circles are said to intersect orthogonally, when the tangents of their points of intersection are at right angles.

2. RADICALAXIS

The locus of the points from which the tangents drawn to two circles are equal is called the RADICAL AXIS of the two circles.

It can be shown that the radical axis is perpendicular to the line joining the centres of the circle.

3. COAXIAL CIRCLES:

A system of circles are said to be coaxial, when they have a common radical axis, i.e., when the radical axis of each pair of circles of the system is the same.

4. INTERSECTING COAXIAL CIRCLES

If any circle of a coaxial system cuts the radical axis at C and D say, all the circles must pass through C and D, for the tangent to the one circle from C (or D) is of zero length, and therefore the tangent from C (or D) to each circle of the system must be of zero length.

In the same way, if any two circles of the system intersect at C and D , all the circles must pass through C and D, and CD is their common radical axis.

5. NON INTERSECTING COAXIAL CIRCLES

We will now consider a construction for a system of coaxal circles for the case in which no circle of the system cuts the radical axis (and no two circles of the system cut one another).

Suppose we have a radical axis and one circle of the system. From N, draw a tangent NQ to the circle. With centre N and radius NQ describe a circle. Draw BR a tangent to this circle from any suitable point in AN (or that line produced). Then the circle with B as centre and BR as radius will be a circle of the system.

For $AN^2 - AQ^2 = NQ^2 = NR^2 = BN^2 - BR^2$

6. LIMITING POINTS

It is obvious from the method of constructing non - intersecting coaxal circles (and also from the relation $AN^2 - AQ^2 = BN^2 - BR^2$) that B cannot be within the construction circle, but may be anywhere else along the line through A and N .

The circles of the system whose centres are at the points L and L' where the construction circle cuts the line AN have zero radius, i.e., are point circles. L and L' are called the limiting points of the system.

A system of intersecting coaxal circles has no real limiting points.

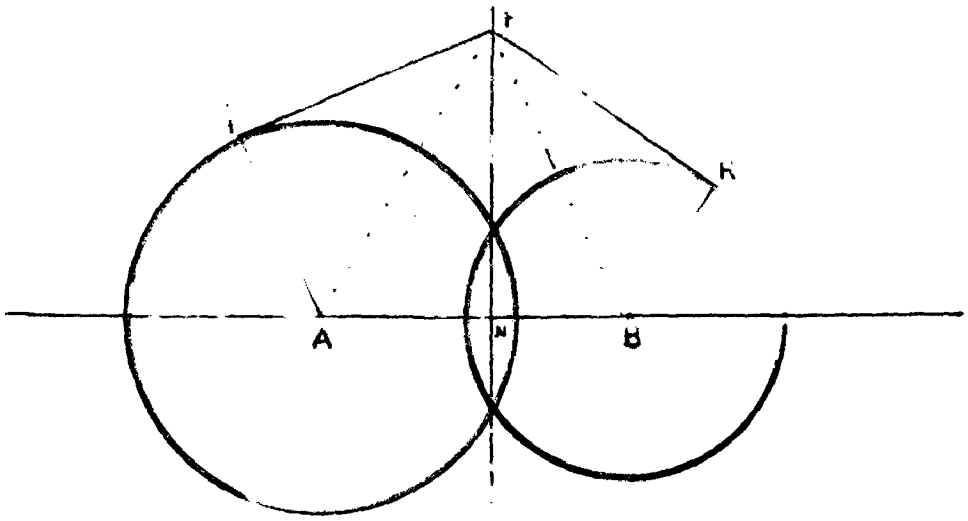

$PQ^2 : PR^2$

$AN^2 - BN^2 = AQ^2 - BR^2$

FIG 2-A

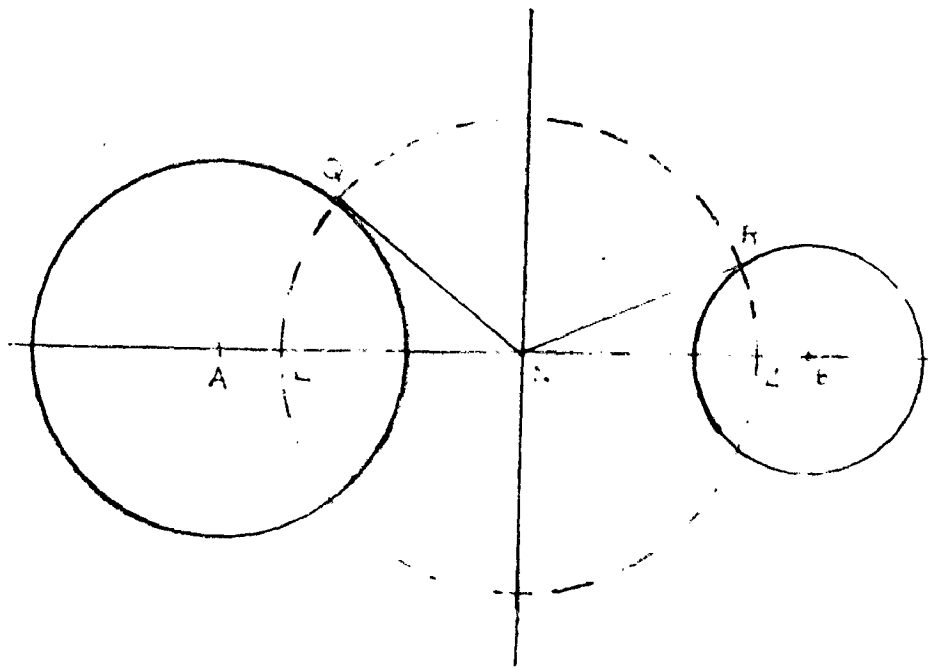

FIG 2-B

7. THEOREM

WITH EVERY SYSTEM OF COAXAL CIRCLES THERE IS ASSOCIATED ANOTHER SYSTEM OF COAXAL CIRCLES, AND EACH CIRCLE OF EITHER SYSTEM CUTS EVERY CIRCLE OF THE OTHER SYSTEMS ORTHOGONALLY.

Since the tangents to a system of coaxal circles (A) from any point P on their radical axis are equal to one another, it follows that the circle (B) with centre P and any one of these tangents as radius will cut all the circles of the system (A) orthogonally.

Again, since there is an infinite number of positions of P on the radical axis, there is an infinite number of circles (B) each of which cuts all the circles of the system (A) orthogonally.

We have still to show that these cutting circles (B) form another coaxal system.

Consider any one circle of the system (A); the tangents from its centre to the orthogonal circles are each a radius of the (A) circle, and therefore equal to one another; similarly for any other circle of the system (A).

∴ The orthogonal circles (B) are coaxal, their radical axis being the line of centres of the system (A).

--

APPENDIX 3.

From Fig. 2.2, we have

$$z - m = r_2 e^{j\theta_2}$$

$$z + m = r_1 e^{j\theta_1}$$

$$\therefore \quad w = u + j v = k \frac{z - m}{z + m}$$

$$u + jv = k \frac{r_2}{r_1} e^{j(\theta_2 - \theta_1)}$$

$$\therefore \quad u = k \frac{r_2}{r_1} \text{Cos} (\theta_2 - \theta_1)$$

$$u = k \frac{r_2}{r_1} \text{Cos } L$$

$$\frac{r_1}{r_2} = \frac{k}{u} \text{Cos } L$$

$$= \text{Constant on } S_1$$

$$= K \text{ (say)}$$

APPENDIX 4

Referring to Fig. 4-A , it can be shown that the tangents drawn from any point on the radical axis to the co-axial circles is of equal length.

i.e $PO^2 = PR^2$

Or $(PC_2)^2 - (R_o)^2 = (PC_1)^2 - (R_1)^2$

$\therefore (PC_2)^2 - (PC_1)^2 = (R_o)^2 - (R_1)^2$

OR $(OC_2)^2 - (OC_1)^2 = R_o^2 - R_1^2$ ...(1)

But $OC_2 = OC_1 + \lambda$ ...(2)

From equations (1) and (2), we have

$\therefore (OC_1 + \lambda)^2 - (OC_1)^2 = R_o^2 - R_1^2$

$$\therefore OC_1 = \frac{R_o^2 - R_1^2 - \lambda^2}{2\lambda}$$

$$\text{or } OC_1 = \frac{1}{2}\left[\frac{R_o^2 - R_1^2}{\lambda} - \lambda\right] \quad \ldots(3)$$

$$\therefore OC_2 = \frac{1}{2}\left[\frac{R_o^2 - R_1^2}{\lambda} + \lambda\right] \quad \ldots(4)$$

Also $(PB)^2 = (PR^2)$

..

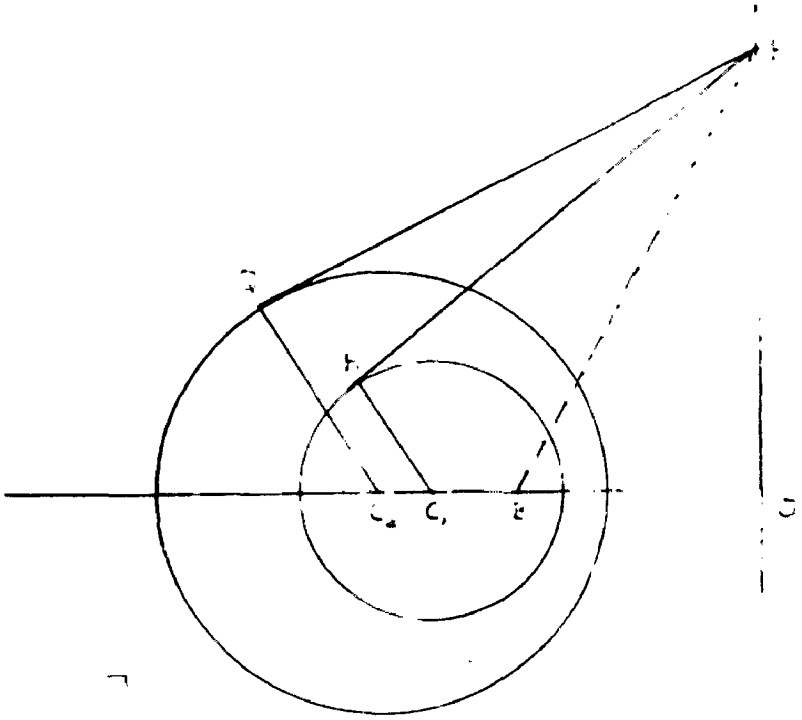

F.G 4-A

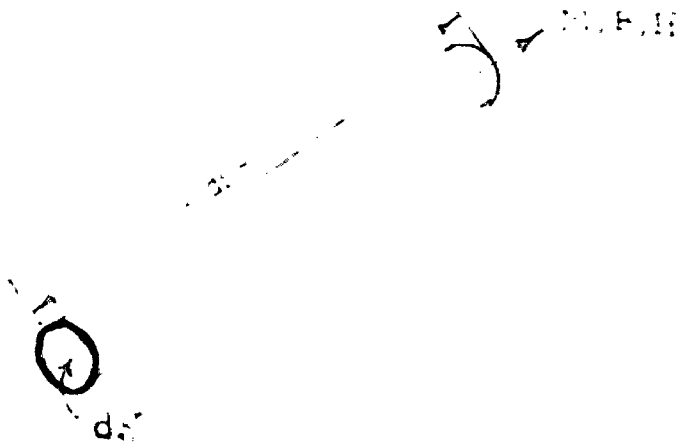

F.G 7-A

$$\therefore \quad OB^2 + OP^2 = PC_1^2 - R_1^2 = OC_1^2 + OP^2 - R_1^2$$

$$\therefore \quad OB^2 = OC_1^2 - R_1^2$$

$$\therefore \quad m^2 = \frac{1}{4}\left[\frac{R_0^2 - R_1^2}{r} - r\right]^2 - R_1^2 \qquad \ldots (5)$$

--

APPENDI

(a) We have

$$K e^{-jL} = \frac{x_1 + m + r}{x - m + r}$$

OR $K \cos L - j K \sin L = \frac{a}{b}$

Where $a = x_1 + m + r \cos \theta$

$b = x_1 - m + r \cos \theta$

Multiplying N_r D^r or of Equ

we have

$$K \cos L - jK \sin L = \frac{ab + r^2}{}$$

$$\therefore \quad K \cos L = \frac{ab + r^2 S_1}{b^2 + r^2}$$

$$K \sin L = \frac{(a-b)\, r}{b^2 + r^2 S_1}$$

Dividing equation No. (4) b

$$\text{Tan } L = \frac{(a-b)\, r\, S_1}{ab + r^2 S_1}$$

$$\text{Tan } L = \frac{2 mr \sin \theta}{x_1^2 - m^2 + 2 x_1}$$

$$\text{Tan } L = \frac{2 m r S_1}{R_1^2 + r^2}$$

$$\therefore L = \mathrm{Tan}^{-1} \frac{2 mr \sin\theta}{R_1^2 + r^2 + 2 x_1 r \cos\theta} \qquad \ldots(5)$$

$$\therefore \cos L = \frac{R_1^2 + r^2 + 2x_1 r \cos\theta}{\left[(R_1^2 + r^2 + 2x_1 r \cos\theta)^2 + (2mr\sin\theta)^2 \right]^{1/2}} \qquad \ldots(6)$$

From equation No. (3) and (6), we have

$$K = \frac{1}{\cos L} \frac{(x_1 + r\cos\theta)^2 - m^2 + r^2\sin^2\theta}{(x_1 + r\cos\theta)^2 + m^2 + 2m(x_1 + r\cos\theta) + r^2\sin^2\theta}$$

$$K = \frac{(m + x_1)^2 + 2(m + x_1) r \cos\theta + r^2}{\left[(R_1^2 + r^2 + 2x_1 r \cos\theta)^2 + (2mr\sin\theta)^2 \right]^{1/2}} \qquad \ldots(7)$$

b) At the rotor surface $r = R_1$

$$\therefore L = \mathrm{Tan}^{-1} \frac{m \sin\theta}{R_1 + x_1 \cos\theta} \qquad \ldots(8)$$

Put $r = R_1$ in equation No. (7)

$$D^r = 2R_1 \left[(R_1 + x_1\cos\theta)^2 + (m\sin\theta)^2 \right]^{1/2}$$

$$= 2R_1 \left[R_1^2 + 2x_1 R_1 \cos\theta + x_1^2 \cos^2\theta + m^2 \sin^2\theta \right]^{1/2}$$

$$= 2R_1 \left[R_1^2 + 2x_1 R_1 \cos\theta + x_1^2\sin^2\theta + x_1^2 \cos^2\theta - R_1^2\sin^2\theta \right]^{1/2}$$

$$= 2R_1 \left[R_1^2 \cos^2\theta + 2x_1 R_1 \cos\theta + x_1^2 \right]^{1/2}$$

$$= 2R_1 (x_1 + R_1 \cos\theta)$$

$$N^2 = m^2 + x_1^2 + 2\,m\,x_1 + 2\,m\,R_1\cos\theta + 2\,x_1 R_1\cos\theta + R_1^2$$

$$= 2\,(x_1 + m)(x_1 + R_1\cos\theta)$$

$$\therefore \quad K\Big|_{\text{at } r = R_1} = \frac{2\,(x_1 + m)(x_1 + R_1\cos\theta)}{2\,R_1\,(x_1 + R_1\cos\theta)}$$

$$= \frac{x_1}{R_1} + \frac{m}{R_1}$$

Since $x_1^2 = m^2 + R_1^2$

$$K\Big|_{\text{at } r = R_1} = \frac{m}{R_1} + \left[1 + \left(\frac{m}{R_1}\right)^2\right]^{1/2} = K_1$$

APPENDIX 6

(a) DETERMINATION OF dK/ds_2

Fig 6A is lettered to correspond to Fig. 3.3, The length AB(=2m) being represented by a.

Since $\frac{r_1}{r_2} = K$

$$\therefore dr_1 = K\,dr_2 + r_2 dK \qquad \ldots(1)$$

.. Since $\theta_2 - \theta_1 = L$ $\qquad \ldots(2)$

$$\therefore d\theta_2 = d\theta_1 \qquad \ldots(3)$$

Again $r_1 \sin\theta_1 = r_2 \sin\theta_2$ $\qquad \ldots(4)$

and $r_1\cos\theta_1 - r_2\cos\theta_2 = a$ $\qquad \ldots(5)$

From Equation No. (5), we have

$$dr_1 \cos\theta_1 - dr_2\cos\theta_2 = r_1\sin\theta_1 d\theta_1 - r_2\sin\theta_2 d\theta_2 = 0 \qquad \ldots(6)$$

From Equation No. (4) and (5) we get,

$$\cos\theta_2 = \frac{r_1^2 - r_2^2 - a^2}{2ar_2}$$

$$\cos\theta_1 = \frac{r_1^2 - r_2^2 + a^2}{2ar_1}$$

$$\therefore (r_1^2 - r_2^2 + a^2)\frac{dr_1}{r_1} = (r_1^2 - r_2^2 - a^2)\frac{dr_2}{r_2} \qquad \ldots(7)$$

From Equations (1) and (7), we get

$$dr_1 = -(r_1^2 - r_2^2 - a^2)\,r_2\,\frac{dK}{2a^2}$$

$$dr_2 = -(r_1^2 - r_2^2 + a^2)\,r_2\,\frac{dK}{2a^2K}$$

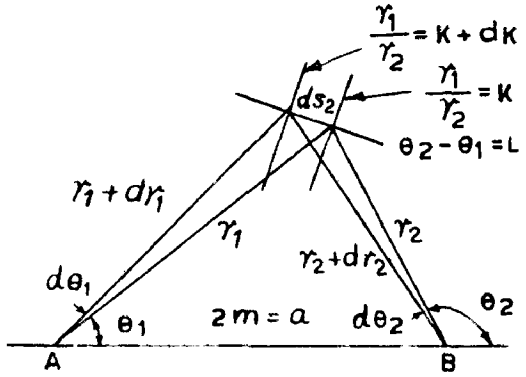

FIG. 6-A. DETERMINATION OF dK/ds_2

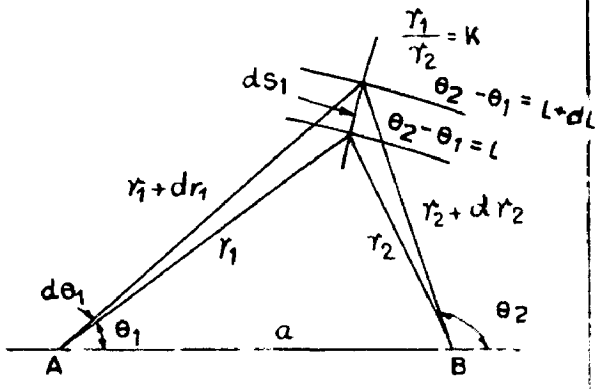

FIG. 6-B. DETERMINATION OF dL/ds_1

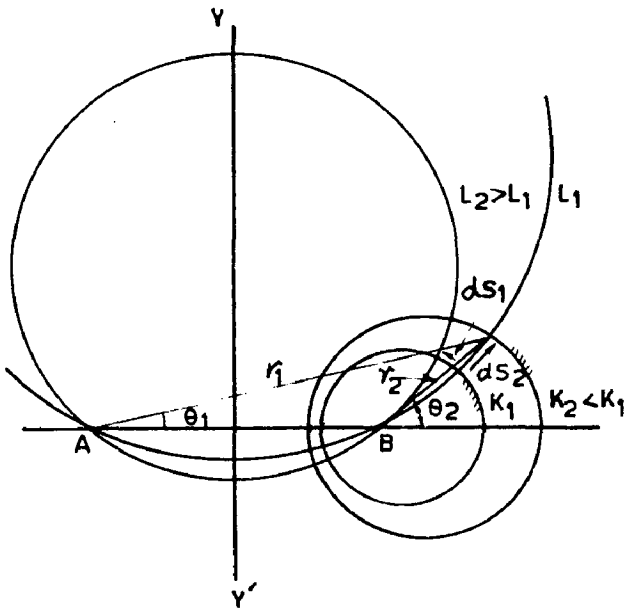

FIG. 6-C. DETERMINATION OF ALGEBRAIC SIGNS OF dK/ds_2 AND dL/ds_1

Also $(dS_2)^2 = (dr_2)^2 + (r_2 d\Theta_2)^2 = dr_1^2 + (r_1 d\Theta_1)^2$

Where $dS_2^2 = (dS_2)^2$, etc.

$$\therefore \quad \frac{d\Theta_1^2}{d\Theta_2^2} = \frac{(dS_2^2 - dr_1^2) / r_1^2}{(dS_2^2 - dr_2^2) / r_2^2} = 1$$

Hence $dS_2^2 = (r_1^2 dr_2^2 - r_2^2 dr_1^2) / r_1^2 - r_2^2$ .....(8)

From Equations (1), (7) and (8), we get

$$\frac{dS_2}{dK} = \pm \frac{3m}{r_2^2} \qquad ...(9)$$

b) DETERMINATION OF $\frac{dL}{dS_1}$:-

Fig. 6-B is lettered to correspond to Fig. 3.2

$$\Theta_2 = \Theta_1 = L$$

$$d\Theta_2 = d\Theta_1 = dL$$

Also $$K = \frac{r_1}{r_2} = \frac{r_1 + dr_1}{r_2 + dr_2}$$

i.e. $r_2 d r_1 = r_1 d r_2$ ....(10)

As before

$$dr_1 \text{Cos}\, \Theta_1 - dr_2 \text{Cos}\, \Theta_2 = r_1 \text{Sin}\, \Theta_1\, d\Theta_1 - r_2 \text{Sin}\, \Theta_2 d\Theta_2$$

$$= - r_1 \text{Sin}\, \Theta_1\, dL$$

Also $$\left(\frac{1}{r_2}\right) \text{Sin}\, \Theta_1 = \frac{1}{a} \text{Sin}\, L$$

Hence

$$(r_1^2 - r_2^2 + a^2)\, dr_1/2ar_1 - (r_1^2 - r_2^2 - a^2)\, dr_2/2ar_2$$

$$= -\left(\frac{r_1 r_2}{a}\right) \text{Sin } L\, dL \qquad \ldots(11)$$

From equations (10) and (11), we have

$$dr_1 = -(r_1^2 r_2/a^2) \text{ Sin } L\, dL$$

$$dr_2 = -(r_1 r_2^2/a^2) \text{ Sin } L\, dL \qquad \ldots(12)$$

Again Since $r_1 \text{Sin } \Theta_1 = r_2 \text{Sin } \Theta_2$

$$\therefore \frac{d\Theta_1}{d\Theta_2} = \frac{\text{Cos } \Theta_2}{K \text{ Cos } \Theta_1}$$

$$\frac{d\Theta_1^2}{d\Theta_2^2} = \frac{1}{K^2} \left(\frac{r_1^2 - r_2^2 - a^2}{2ar_2}\right)^2 \Big/ \left(\frac{r_1^2 - r_2^2 + a^2}{2ar_1}\right)^2$$

Therefore, as in 'a)

$$\begin{pmatrix} (dS_1^2 - dr_1^2)/r_1^2 \\ (dS_2^2 - dr_2^2)/r_2^2 \end{pmatrix} = \begin{pmatrix} r_1^2 - r_2^2 - a^2 \\ r_1^2 - r_2^2 + a^2 \end{pmatrix}^2$$

Which on simplification gives -

$$dS_1^2 = \frac{(r_1^2 - r_2^2 + a^2)^2 - (r_1^2 - r_2^2 - a^2)^2}{(r_1^2 - r_2^2 + a^2)^2 r_2^2 - (r_1^2 - r_2^2 - a^2)^2 r_1^2} r_1^2 dr_2^2 \qquad \ldots(13)$$

$$\text{Also } \text{Sin}^2 L = 1 - \frac{(r_1^2 + r_2^2 - a^2)^2}{(2r_1 r_2)^2} \qquad \ldots(14)$$

By aid of Equation (17) and (16), Equation (13) is reduced to the form

$$ds_1^2 = \left(\frac{r_1^2 r_2^2}{r^2}\right) d\theta^2$$

$$\therefore \quad \frac{d\theta}{ds_1} = \pm \frac{2}{K r_2^2} \qquad \ldots(18)$$

The correct sign of equations (9) and (18) is discussed below :-

a) ALGEBRAIC SIGNS OF $\frac{dK}{ds_2}$ AND $\frac{d\theta}{ds_1}$:-

The signs of both $\frac{dK}{ds_2}$ and $\frac{d\theta}{ds_1}$ as determined above are ambiguous since each formula is obtained by evolution. The ambiguity may be removed in any specific case by assigning positive directions to ds_1 and ds_2

Referring to Fig. C-C , K_1 and K_2 represents the rotor and the stator circles respectively, and L_1 , L_2 are the members of the orthogonal system L = Constant . Since $K = r_1 / r_2$ it is clear that the magnitude of K diminishes as the diameter of the circle increases. Hence it is infinitely small at the limiting point D and is equal to the unity on the line $T T'$, which is derived from the system K = constant by making the diameter indefinitely great. Hence defining the positive direction of ds_2 as indicated, i.e. in the positive direction of r , it follows that dK / ds_2 is negative.

Again since $L = \theta_2 - \theta_1$, it is evident that L_2 L_1 . Hence, with positive direction of dS_1 as shown, i.e. in the positive direction of θ it follows that $\frac{dL}{dS_1}$ is positive.

APPENDIX - 7

MAXWELLIAN STRESSES

The force on a piece of magnetic substance carrying a current may for convenience of calculation be divided into two parts :

i. The force on the element in consequence of the presence of the currents, and

ii. The force due to magnetization in the element, the force due to currents being now ignored.

To compute (i), we have that the resolved components of the force in the x direction due to currents alone is,

$$J_y B_z = J_z B_y \qquad \ldots(1)$$

per unit volume

J = Current density in the element

B = the flux density at the element.

To compute (ii) consider an elemental cylinder of length ds and area of the section dS of the material as shown in Fig. (7A) page No. . The axis is so chosen that the axis is along the line of induction B. The pole strength of this elemental magnet is MdS. Therefore, the force on the south pole in the x direction is $- H_x M dS$, whilst the force on the north pole is $\left(H_x + \frac{\partial H_x}{\partial x} dx \right) M dS$. Hence the net force on this elemental volume in the x - direction is

$$\left(\frac{\partial H_x}{\partial z} \, dz \right) \text{and}$$

$$= \left[\frac{\partial H_x}{\partial x} \cdot \frac{dx}{dz} + \frac{\partial H_x}{\partial y} \cdot \frac{dy}{dz} + \frac{\partial H_x}{\partial z} \cdot \frac{dz}{dz} \right] \text{dv}$$

Where dv is the volume of the cylinder.

Since $\left(\frac{dx}{dz} \right), \left(\frac{dy}{dz} \right)$ and $\left(\frac{dz}{dz} \right)$ are the direction cosines of the axis of magnetisation, the above expression for the x component of the net force per unit volume may be re-written as :

$$M_x \frac{\partial H_x}{\partial x} + M_y \frac{\partial H_x}{\partial y} + M_z \frac{\partial H_x}{\partial z} \qquad \ldots (2)$$

Since Curl H = 0 , (in current free region) , we have

$$\frac{\partial H_x}{\partial y} = \frac{\partial H_y}{\partial x} \quad , \quad \frac{\partial H_x}{\partial z} = \frac{\partial H_z}{\partial x}$$

Thus the x component of force due to the magnetism, ignoring the effects of currents is.

$$M_x \frac{\partial H_x}{\partial x} + M_y \frac{\partial H_y}{\partial x} + M_z \frac{\partial H_z}{\partial x} \qquad \ldots (3)$$

Hence the net for per unit volume in the x direction is given by

$$F_x = M_x \frac{\partial H_x}{\partial x} + M_y \frac{\partial H_y}{\partial x} + M_z \frac{\partial H_z}{\partial x} + (J_y B_z - J_z B_y) \qquad \ldots (4)$$

To eliminate , H's we have

$$B = \frac{1}{\mu_0} (B - M)$$

or $M_x = B_x - \mu_0 H_x$

$M_y = B_y - \mu_0 H_y$

$M_z = B_z - \mu_0 H_z$

Thus,

$$F_x = B_x \frac{\partial H_x}{\partial x} + B_y \frac{\partial H_y}{\partial x} + B_z \frac{\partial H_z}{\partial x}$$

$$- \frac{\mu_0}{2} \frac{\partial}{\partial x} (H_x^2 + H_y^2 + H_z^2) + (J_y B_z - J_z B_y)$$

Since

$$H_x \text{ div } B = H_x \frac{\partial B_x}{\partial x} + \frac{\partial B_y}{\partial y} + \frac{\partial B_z}{\partial z} = 0$$

$$\text{and } J_y = \frac{\partial H_x}{\partial z} - \frac{\partial H_z}{\partial x}$$

Substituting and rearranging -

$$F_x = \frac{\partial}{\partial x} H_x B_x - \frac{\mu_0}{2} (H_x^2 + H_y^2 + H_z^2)$$

$$+ \frac{\partial}{\partial y} H_x B_y + \frac{\partial}{\partial z} H_x B_z \quad \ldots (8)$$

In analogy with the theory of elasticity, for an elemental parallelo-piped under subjected to the surface stresses, the x-t component of the force acting in the x- direction is :

$$\frac{\partial P_{xx}}{\partial x} + \frac{\partial P_{xy}}{\partial y} + \frac{\partial P_{xz}}{\partial z} \quad \ldots (8)$$

Where the stresses are -

$$P_{xx} \quad P_{xy} \quad P_{xz}$$
$$P_{yx} \quad P_{yy} \quad P_{yz}$$
$$P_{zx} \quad P_{zy} \quad P_{zz}$$

The surfaces P_{xx}, P_{xy}, P_{xz} are the stresses acting on a surface perpendicular to the x- axis. P_{xx} being the component along the x- direction, P_{xy} the component along the y-direction, and P_{xz} along the z- direction and so on .

Comparing equations (3) and (6), it is seen that

$$P_{xx} = H_x B_x = \frac{\mu_0}{2} (H_x^2 + H_y^2 + H_z^2)$$

$$P_{xy} = H_x B_y$$

$$P_{xz} = H_x B_z$$

Similarly for others, if H and B were to be in the same direction then choosing the x- axis along B we have

$$B_y = B_z = 0 \text{ and } H_y = H_z = 0$$

$$P_{xx} = HB = \frac{1}{2} \mu_0 H^2$$

$$P_{yy} = -\frac{\mu_0}{2} H^2$$

$$P_{zz} = -\frac{\mu_0}{2} H^2$$

The rest of the stresses being zero.

Hence we can say that the medium is in a static of stress having -

i. a tensile stress of magnitude $BH - \frac{\mu_o}{2} H^2$ newtons per square meter along the line of force at each point.

ii. a compressive stress $\frac{1}{2}\mu_o H^2$ Newtons per square meter in every direction at right angle to the line of force at each point.

---0:0:0---